



Published in final edited form as:

J Med Chem. 2009 July 9; 52(13): 4038–4053. doi:10.1021/jm900356n.

Synthesis and Electrochemistry of 2-Ethenyl and 2-Ethanyl Derivatives of 5-Nitroimidazole and Antimicrobial Activity against *Giardia lamblia*

Carlos A. Valdez^{†,§}, Jonathan C. Tripp^{†,§}, Yukiko Miyamoto[‡], Jaroslaw Kalisiak[†], Petr Hruz[‡], Yolanda S. Andersen[‡], Sabrina E. Brown[⊥], Karina Kangas[⊥], Leo V. Arzu[⊥], Barbara J. Davids[‡], Frances D. Gillin[‡], Jacqueline A. Upcroft^{||}, Peter Upcroft^{||}, Valery V. Fokin[†], Diane K. Smith[⊥], K. Barry Sharpless[†], and Lars Eckmann^{*,‡}

Department of Chemistry and The Skaggs Institute for Chemical Biology, The Scripps Research Institute, 10550 North Torrey Pines Road, La Jolla, California 92037, Departments of Medicine and Pathology, University of California–San Diego, La Jolla, California 92093, Department of Chemistry and Biochemistry, San Diego State University, San Diego, California 92182, and The Queensland Institute of Medical Research, 300 Herston Road, Brisbane, Australia

Abstract

Infections with the diarrheagenic pathogen, *Giardia lamblia*, are commonly treated with the 5-nitroimidazole (5-NI) metronidazole (Mz), and yet treatment failures and Mz resistance occur. Using a panel of new 2-ethenyl and 2-ethanyl 5-NI derivatives, we found that compounds with a saturated bridge between the 5-NI core and a pendant ring system exhibited only modestly increased anti-giardial activity and could not overcome Mz resistance. By contrast, olefins with a conjugated bridge connecting the core and a substituted phenyl or heterocyclic ring showed greatly increased anti-giardial activity without toxicity, and several overcame Mz resistance and were more effective than Mz in a murine giardiasis model. Determination of the half-wave potential of the initial one-electron transfer by cyclic voltammetry revealed that easier redox activation correlated with greater anti-giardial activity and capacity to overcome Mz resistance. These studies show the potential of combining systematic synthetic approaches with biological and electrochemical evaluations in developing improved 5-NI drugs.

Introduction

The anaerobic protozoan parasite, *Giardia lamblia*, is a major cause of human diarrheal disease, infecting an estimated 10% of the world's population in both endemic and epidemic fashion.¹ In the U.S., *Giardia* is the most common cause of waterborne diarrheal disease, with international travelers, hikers, and children in day care centers at particular risk.² Infection is by fecal–oral transmission and is initiated by ingestion of infectious cysts in contaminated water or through person-to-person contact. After excystation, flagellated trophozoites colonize the upper small intestine where they attach to the epithelial lining but do not invade the mucosa. The duration of giardial infection is variable, but chronic infection and reinfection occur commonly.³ Although ~50% of *Giardia* infections are asymptomatic, major symptoms include

*To whom correspondence should be addressed. Phone 858-534-0683. Fax: 858-534-3338. leckmann@ucsd.edu.

[†]The Scripps Research Institute.

[§]These authors contributed equally to this work.

[‡]University of California–San Diego.

[⊥]San Diego State University.

^{||}The Queensland Institute of Medical Research.

diarrhea, often severe and protracted, with malabsorption, dehydration, weight loss, failure to thrive, cognitive impairment in children, and chronic fatigue in adults.^{4,5} These symptoms result from a combination of intestinal villus atrophy, loss of brush border microvilli, digestive enzyme deficiencies, and epithelial barrier dysfunction.^{6,7}

The leading anti-giardial agent, metronidazole (Mz, Figure 1), is a synthetic 5-nitroimidazole (NI) derivative introduced in 1959 by Rhône-Poulenc. In addition to *Giardia*, Mz is active against *Entamoeba histolytica* and *Trichomonas vaginalis*, as well as several clinically important anaerobic bacteria (including *Clostridium difficile*, *Helicobacter pylori*, and *Bacteroides fragilis*), making it a highly versatile antibiotic. Mz has a long record of efficacy and safety.^{8,9} On the basis of the therapeutic utility of Mz, several other 5-NIs^a have been developed more recently. For example, tinidazole (**1**, Figure 1) is a N1-position modified 5-NI, which has been approved by the FDA for the treatment of giardiasis. Not all anti-giardial nitro drugs are based on the 5-NI scaffold. Nitazoxanide (**2**, Figure 1) belongs to an emerging class of 5-nitrothiazole compounds with potent anti-giardial activity,¹⁰ although *Giardia* lines resistant to Mz are cross-resistant to nitazoxanide.⁹ Overall, Mz remains the standard treatment for giardiasis to date, making the discovery and development of new therapeutics an important goal in expanding the arsenal of antibiotics for controlling the infection.

The high specificity of the 5-NIs is due to the requirement for the prodrug to be reduced to toxic free radical intermediates by low redox potential reactions present only in anaerobic microbes.¹¹ These short-lived free radicals cause lethal damage to the microbe, although their cellular targets are not well-defined in either eukaryotes or prokaryotes. Energy metabolism in *Giardia*, which does not have mitochondria, is fermentative, and electron transport proceeds in the absence of oxidative phosphorylation present in organisms with mitochondria. However, *Giardia* is microaerotolerant and can reduce O₂ and thus protect the highly oxygen-sensitive, key metabolic enzyme pyruvate-ferredoxin oxidoreductase and the iron-containing ferredoxins that activate Mz.¹² The oxidoreductase carboxylates pyruvate and donates electrons to ferredoxin, which in turn reduces other components in the electron transport chain. ATP production is linked to pyruvate decarboxylation.¹³ Reduced ferredoxin activates the critical nitro group of the prodrug Mz, leading to formation of toxic free radicals that kill the parasite. Selective reductive activation in the target microbes, but not mammalian cells, is generally thought to be critical for the potency and selectivity of 5-NI drugs.¹⁴ However, relatively little is known about the electrochemical properties of most 5-NIs, making it difficult to draw detailed conclusions about the importance of low redox potential for their antimicrobial activity, selectivity, and mechanisms of action.

In spite of the efficacy of 5-NI drugs, treatment failures in giardiasis occur in up to 20% of cases.¹⁴ Clinical resistance of *G. lamblia* to Mz and other 5-NIs is proven, and in vitro resistance can be induced so that parasites grow in physiologically relevant concentrations of Mz.¹⁵ In addition, resistance has been induced in vitro against all commonly used anti-giardial drugs, including different 5-NIs, furazolidone, albendazole, and quinacrine,^{9,14} further demonstrating the need for new compounds to preempt resistance development. Prior studies suggested that modifications in the 2-position of the imidazole ring can lead to effective 5-NI drugs.^{16,17} For example, the 2-position modified 5-NI compound **3** (Figure 1, compound **17** in ref ¹⁶) is very active against *G. lamblia* and can overcome Mz resistance.¹⁶ Although these 5-NI derivatives were not examined for their toxicity, in vivo efficacy, or mechanisms of action, they raised the possibility that 2-position derivatives of 5-NI may be promising for developing new, potent, and safe drugs against giardiasis.

^aAbbreviations used: CV, cyclic voltammogram; E_{1/2}, half-wave potential; E_p, peak potential; Mz, metronidazole; NI, nitroimidazole.

In the present study, we synthesized a library of substituted 2-styryl 5-NI compounds and evaluated the significance of the olefin bridge directly attached to the NI ring by chemically modifying it by dibromination, dihydroxylation, and reduction. These new compounds were assessed for their potency against *G. lamblia* in vitro and in vivo, their cytotoxicity in human cells, and their electrochemical properties.

Results and Discussion

Chemistry

We synthesized 2-styryl 5-NI derivatives using the aldol condensation¹⁸ between 1,2-dimethyl-5-nitroimidazole (dimetridazole, **4**; Table 1) and a panel of aryl aldehydes in the presence of sodium ethoxide in ethanol as shown in Table 1. By use of this protocol, a diverse array of functionality was incorporated into the 2-position of the NI core ranging from electron-rich aromatic systems (Table 1, entries 2–5, 16, and 18) and electron-poor ones (entries 6–15 and 17) to different heterocyclic scaffolds (entries 23–27). Because certain halogen substitutions in the aromatic ring can yield potent antimicrobial compounds,^{16,17} we systematically explored most of the possible halogen monosubstitutions around the phenyl ring (entries 6–15). While the yields of these reactions varied widely (13–77%), sufficient material could be produced for biological testing after purification by flash chromatography or recrystallization.

In another round of derivatizations, we functionalized the double bond present in the aldol condensation products. This allowed us to probe the biological importance of an unsaturated bridge connecting the NI and the phenyl ring in the new compounds. To this end, we initially attempted to oxidize the double bond in **5** to the corresponding epoxide **32** using *m*-CPBA (Scheme 1a). Although the epoxide was observed by LCMS, it proved to be difficult to isolate or even capture by treatment of the crude reaction mixture with a suitable nucleophile. A more productive functionalization was achieved by treating olefin **12** with bromine in chloroform to produce tribromide **33** in 88% yield (Scheme 1b). Additionally, the double bonds of nitroimidazoles **8** and **12** were dihydroxylated using the acidic Upjohn procedure¹⁹ to furnish diol **34** in 28% and diol **35** in 14% yield (Scheme 1c). Subsequent acetylation of diols **34** and **35** using acetic anhydride produced compounds **36** and **37** in 66% and 92% yields, respectively (Scheme 1c).

Last, we evaluated the complete reduction of the C2-olefin in the aldol adducts to their saturated counterparts for direct structure–activity comparisons. Reducing the double bond in the presence of the nitro group on the imidazole ring proved difficult. Thus, as expected, hydrogenation of **5** over palladium or platinum catalysts efficiently hydrogenated the double bond but also reduced the nitro group to the corresponding amine **38**, as outlined in Scheme 2a. We also attempted an alkylation strategy where dimetridazole **4** was treated with NaOEt and benzyl bromide but observed no conversion to the desired product (Scheme 2b). A NiCl₂/NaBH₄ reducing agent system,²⁰ which is a mild source of hydride, was also tried with olefin **5** but with unsatisfactory results, as only the fully reduced product **38** was again observed (Scheme 2c). We further explored constructing the imidazole ring independently followed by a nitration to give the desired product.²¹ However, the nitration of known imidazole **39** occurred on the undesired aromatic ring, forcing us to abandon this approach (Scheme 2d). Ultimately, we evaluated diimide as the reducing agent. While a more conventional Cu(II)/hydrazine system²² for generating the diimide failed to effect the reaction, tosyl hydrazine in pyridine²³ selectively reduced the double bond while leaving the nitro functionality intact (Scheme 2e). This procedure allowed us to convert the aldol adducts **5**, **8**, and **12** to their fully saturated counterparts **40**, **41**, and **42** in 32%, 18%, and 17% yields, respectively (Scheme 2e).

Improved Antigiardial Activity and Selectivity of 2-Styryl-5-NI Derivatives

Prior work had demonstrated that dibrominated 5-NI compound **3** (Figure 1), a C2-modified 5-NI, had increased potency against *G. lamblia* relative to Mz.¹⁶ In the present study, utilizing a panel of isolates representing assemblages A and B, the two major genetic groupings that contain all human-infectious *Giardia*, we confirmed that compound **3** (Table 2, entry 1) possessed a 40-fold increased anti*giardia* activity over Mz (Table 2, entry 10). However, toxicity analysis in the human cell line, HeLa, indicated that dibromide **3** was > 500-fold more toxic than Mz. To consider both the potency and toxicity of the new compounds in comparison to Mz, the in vitro selectivity was determined by calculating the ratio of the IC₅₀ in HeLa cells to EC₅₀ in *Giardia* as an estimate for the therapeutic index. The most promising candidate compounds for further evaluation will be ones with an equal or higher in vitro selectivity ratio than Mz. In the case of dibromide **3**, the selectivity ratio was > 10-fold lower than that of Mz (Table 2). Similarly, a close analogue of **3** bearing a bromine instead of a methyl at the phenyl ring para to the saturated bridge, compound **33** (Table 2, Entry 2), did not overcome the toxic effects of **3** and had even lower antimicrobial activity, further reducing the selectivity ratio. To evaluate whether the toxicity of **3** could be attenuated without affecting its potent anti*giardia* activity, we synthesized compounds related to dibromide **3** in which the bromine atoms in the bridge were replaced systematically with hydroxyl groups (**34** and **35**, Table 2, entries 3 and 4) or acetoxy groups (**36** and **37**, Table 2, entries 5 and 6). These compounds also had selectivity ratios markedly below Mz, rendering them significantly less effective than Mz. Finally, we prepared more direct analogues of dibromide **3**, in which the bromine atoms were replaced with hydrogen atoms (**40–42**, Table 2, entries 7–9). Although elimination of the two bromine atoms in **3** decreased toxicity, it also compromised anti*giardia* activity and the selectivity ratio. Together, these results suggest that modifications in the saturated bridge at C2 of the nitroimidazole core could not overcome toxicity without markedly reducing antimicrobial activity.

On the basis of the disappointing results obtained with the C2-saturated bridge analogues, we reasoned that an unsaturated bridge joining the phenyl ring to the 5-NI core might exert more direct electronic influence on the 5-NI ring and improve antimicrobial activity. To explore this idea, we synthesized a series of 5-NI compounds bearing a substituted styryl unit directly attached to the C2 position as presented in Table 1. The simplest compound of this styryl series with a bare phenyl ring, **5** (Table 3, entry 1), displayed strong anti*giardia* activity without measurable toxicity, leading to a high selectivity ratio. Substitutions at the phenyl with one or several methyl moieties (**6–9**, Table 3, entries 2–5) did not improve the activity or selectivity ratio of compound **5**. Similarly, halogen substitutions on the phenyl ring (**10–19**, Table 3, entries 6–15) also did not significantly improve anti*giardia* activity. Toxicity was only very slightly increased by most of these modifications, with the exceptions of the methyl, chloro, and iodo substitutions at the meta position of the phenyl ring, which increased toxicity moderately (**7**, **14**, **18**, Table 3, entries 3, 10, and 14, respectively) but not to the levels of the dibrominated compounds **3** and **33** (Table 2, entries 1 and 2). Addition of larger side chains at the phenyl moiety, including OMe (**20** and **22**, Table 3, entries 16 and 18), OCF₃ (**21**, Table 3, entry 17), and phenyl (**24**, Table 3, entry 20), markedly reduced activity against *Giardia*, while addition of diethoxymethyl (**23**, Table 3, entry 19) did not affect anti*giardia* activity or toxicity. Beyond substituted styryl compounds, we performed the aldol condensation reaction between dimetridazole **4** and a panel of heterocyclic and other aromatic aldehydes to furnish compounds **25–31** (Table 1, entries 21–27). Even though these compounds exhibited promisingly low cytotoxic profiles, their anti*giardia* activity and selectivity ratio (Table 4, entries 1–7) did not surpass that exhibited by the simple phenyl compound **5** (Table 3, entry 1).

Together, these results show that derivatives of 5-NIs bearing an olefin directly attached to the C2 position of the imidazole ring have potent anti-giardial activity. More importantly, most of the analogues possess low cytotoxicity and excellent selectivity ratios comparable to or exceeding that of Mz.

Activity of Selected 5-NIs against *G. lamblia* in a Murine Infection Model

As a next step toward evaluating the ultimate clinical potential of the new 5-NI derivatives, we tested several of the most potent and structurally diverse compounds in a murine model of *G. lamblia* infection. Normal adult mice were infected orally with trophozoites of the GS/M strain of *G. lamblia* and left for 2 days to allow full establishment of infection. Mice were then treated with five doses of the compounds over a 3-day period, and infectious load was assessed by counting the number of live trophozoite in the small intestine. Mz, used as reference drug, caused a ~1000-fold reduction in trophozoite numbers, but not parasite eradication, at a dose of 10 mg/kg, while it had no significant effect at the lower dose of 2 mg/kg (Figure 2). Six of the seven tested new 5-NI derivatives were at least as potent as Mz at 10 mg/kg, with four of them (**5**, **19**, **28**, and **29**) causing complete clearance of the infection. One compound, **12**, had no significant activity at either dose. Two of the four compounds, **19** and **28**, that caused complete eradication at 10 mg/kg showed significant activity at 2 mg/kg, further demonstrating that they were more potent than Mz (Figure 2). None of the compounds had any clinically observable untoward effects on the mice during the 3-day treatment period at the higher dose (10 mg/kg).

Further analysis of the in vivo and in vitro data revealed that the in vitro properties of the compounds only partly predicted their in vivo behavior. While a positive correlation existed between in vitro activity and in vivo potency, several notable exceptions were observed (Figure 2). Compound **12** was the fourth most active in vitro (EC₅₀ of 49 nM, Table 3, Entry 8) of the seven new 5-NI derivatives tested in vivo, and yet it showed no activity in vivo. Conversely, compound **28** was only the fifth most active compound in vitro (EC₅₀ of 76 nM, Table 4, entry 4), but it was one of the two most potent compounds in vivo (Figure 2). Thus, compound **12** relatively underperformed, while compound **28** overperformed, in vivo relative to the respective in vitro activity. Nonetheless, these results indicate that several of the new 5-NI compounds have strong in vivo activity and no apparent acute toxicity, supporting the potential utility of these compounds for clinical applications.

Activity of 2-Position Modified 5-NIs against Mz-Resistant *G. lamblia*

Resistance of *G. lamblia* to Mz has been documented in the laboratory and threatens to become a serious clinical problem.^{9,14} We therefore tested the newly synthesized 5-NIs against two independently derived isogenic pairs of Mz-resistant isolates of *G. lamblia* 713 and *G. lamblia* 106.^{24,25} These lines exhibit stable Mz resistance with 30- and 6-fold respective increases in EC₅₀ in the Mz-resistant line relative to the EC₅₀ in the matched parental line, termed here “Mz resistance ratio” or “EC₅₀ (Mz^R)/EC₅₀ (Mz^S)”, with a lower resistance ratio indicating a greater ability to overcome Mz resistance. Analysis of the data for the two pairs of *G. lamblia* lines revealed that the compounds exhibited a range of resistance ratios (Figure 3A and Table 5). Most of the ratios of these compounds were lower than that of Mz for at least one of the two *G. lamblia* pairs examined, while compounds **5** and **36** were comparable to and compound **40** higher than Mz (Table 5). Importantly, the correlation of resistance ratios between the 713 line and the 106 line was weak, as a substantial number of the compounds we tested overcame Mz resistance in only one line. On the basis of this observation, we divided several of the compounds into three major resistance groups (Figure 3A and Table 5). Group A contained compounds that could substantially overcome Mz resistance in both pairs of *G. lamblia* lines, while compounds in groups B and C could overcome resistance in one of the two pairs but not (or much less so) in the other.

These results provide strong pharmacological evidence for more than one mechanism of Mz resistance in *G. lamblia*. Diversity in antimicrobial resistance mechanism is not surprising, given that the *Giardia* lines were derived independently,^{24,25} and is well recognized for other antimicrobials and microbes.^{26,27} Moreover, different resistance mechanisms have been proposed for *G. lamblia*, including the down-regulation of the critical pathway required for reductive 5-NI drug activation,^{13,28,29} although the full extent and relative importance of different resistance mechanisms remain elusive. In any case, the existence of group A compounds suggests that it is possible to develop 5-NIs that can markedly overcome at least two forms of Mz resistance and may be active against other forms of Mz resistance in *G. lamblia*.

In searching for properties that might explain the resistance grouping of the compounds, we found that the ability to overcome Mz resistance was not correlated with the potency of the respective compounds (Figure 3B). For example, two group A compounds, **9** and **19**, exhibited comparable improvements (i.e., decreases) in resistance ratios in both *G. lamblia* pairs, but compound **9** had ~10-fold lower EC₅₀ against the respective Mz-sensitive parental lines (Table 5). Moreover, compounds **11** and **5** had comparable activities against the Mz-sensitive lines but were markedly different in their resistance profiles (Table 5). Structural analysis also did not reveal any clear explanation for the resistance grouping of the compounds, although some interesting connections could be discerned. For example, among the 2-styryl 5-NIs, two of the four group A compounds (**11** and **19**) possessed a substitution (i.e., Br and F) at the meta-position in the ring while none of the five group B or C phenyl-carrying styryl compounds did. The importance of the substitution position is illustrated by the set of Br-substituted compounds, **10** (ortho), **11** (meta), and **12** (para). The *m*-Br containing compound (**11**, group A) showed excellent improvements in resistance ratios for both *G. lamblia* pairs, while the *o*-Br substitution (**10**, group B) improved the ratio in the 713 line but not the 106 line, and the *p*-Br substitution (**12**, group C) improved the ratio in the 106 line but less so in the 713 line (Table 5). On the other hand, these structure–activity relationships did not apply uniformly for other substituents. For example, while the *o*-Br and *p*-Br substituted compounds fell distinctly into groups B and C, respectively, the same was not true for the Cl substitutions, where the ortho and para substituted compounds (**13** and **15**, respectively) had very similar resistance profiles (Table 5). Overall, these results demonstrate that several of the new 5-NIs can markedly, albeit not entirely, overcome resistance to Mz in *G. lamblia*. However, the ability to do so is not readily predictable on the basis of overall anti-giardial activity or structural features.

Electrochemical Properties of 5-NI Alkenes and Alkanes under Anhydrous Conditions

Since structural features of the newly synthesized compounds did not provide consistent explanations for the compounds' antimicrobial activities, we began to explore their electrochemical properties, since NIs are prodrugs that must be activated by reduction in the target microbes before they exhibit antimicrobial activity. We reasoned that chemical modification of the molecule with groups that perturb the electronic properties of the NI ring would affect the ease with which these molecules undergo reduction. The redox potential of Mz is more negative than the lowest redox couple in mammalian cells, which is believed to be the basis for its high specificity and low toxicity. To determine whether differences in redox activation might explain the ability of the different 5-NIs to overcome Mz resistance, we measured the half-wave potential ($E_{1/2}$) of the initial one-electron transfer reaction (0/−1 reduction) for groups A, B, and C compounds and selected additional compounds. Measurements were done by cyclic voltammetry in DMSO under anhydrous conditions, with ferrocene as an internal standard and reference point for measuring $E_{1/2}$.

Representative cyclic voltammograms (CVs) under these conditions for Mz and one of the new 5-NIs, the 3-thiophene compound **31**, are shown in Figure 4A. From the similarity of the CVs it can be deduced that both compounds exhibited a similar electrochemical behavior, corresponding to a reversible one-electron reduction to the radical anion. The $E_{1/2}$ of Mz was -1.561 V under these experimental conditions, which was very close to the $E_{1/2}$ of -1.557 V for 1-methyl-5-NI, the unsubstituted parent compound of all the new 2-substituted *N*-methyl-5-NI (Table 6). Most of the new 5-NIs we assayed had more positive $E_{1/2}$, indicating that they could be reduced more readily, whereas six compounds exhibited more negative $E_{1/2}$ than Mz and 1-methyl-5-NI (Table 6).

Three of these six compounds had a C2-saturated bridge between the two ring systems (**40–42**). This is consistent with the electron-donating ability of alkyl groups, which add electron density to the nitroimidazole ring, making reduction more difficult. Since there is no conjugation connecting the imidazole ring to the pendant phenyl ring, substitution on the phenyl ring had no significant effect on the $E_{1/2}$ (Table 6). The exception to this notion were the two 5-NI alkanes, **3** and **33**, both of which showed much more positive $E_{1/2}$ than Mz (Table 6). However, both compounds had di-Br substitutions in the C2-saturated bridge and showed more complicated electrochemical behavior with an irreversible reduction peak in the CV leading into and overlapping with a reversible wave. The irreversible peak was likely associated with reductive removal of the Br and the reversible wave with reduction of the product NI. Interestingly, both compounds were quite toxic in HeLa cells (Table 2, entries 1 and 2), suggesting that their easier reduction at less negative redox potentials, or their redox-induced structural change and probable side chain release, might contribute to toxicity.

All of the other tested compounds with significantly more positive $E_{1/2}$ (ranging from 30–90 mV) than Mz and 1-methyl-5-NI were C2-olefinic derivatives of 5-NI, suggesting that the conjugation through the unsaturated link between the imidazole ring and the pendant aromatic ring stabilizes the radical anion through delocalization and thereby favors reduction of the nitro group. The compounds substituted with phenyl (**5**), methylphenyl (**6–8**), and trimethylphenyl (**9**) had 30–50 mV more positive $E_{1/2}$ than Mz (Table 6). Extended conjugation with larger aromatic groups (**24–26**) and/or heterocycles with electronegative elements (N, O) (**28** and **29**) made the compounds easier to reduce (50–65 mV more positive $E_{1/2}$ than Mz) than the methylphenyl or phenyl derivatives, as did addition of electron-withdrawing halogen groups on the phenyl ring (55–90 mV more positive than Mz). The easiest compound to reduce in this series was **16**, which has two electron-withdrawing chlorines on the phenyl ring, giving it a ~ 90 mV more positive $E_{1/2}$ than Mz (Table 6).

To gain a better understanding of the observed electrochemical properties of the different 5-NI compounds, we evaluated the substituent effects on the redox potentials using Hammett plots.^{30–33} In this analysis of aromatic compounds, the $E_{1/2}$ of a series of meta- and para-substituted derivatives are plotted against the Hammett σ values. The latter are derived from the acid dissociation constants of substituted benzoic acids and provide a quantitative measurement of the electron-donating/accepting character of a particular substituent. Figure 4B shows the Hammett plot for the 2-alkenylphenyl compounds that have simple meta or para substituents for which good σ values are available.³⁴ As expected, we observed an approximately linear correlation with a positive slope, indicating stabilization of negative charge. This correlation suggests that the C2-olefin bridge provides an electronic communication between the pendant phenyl ring and the NI. Dividing the slope of this type of Hammett plot by the Nernst equation coefficient of 0.0592 V yields a dimensionless parameter that is directly comparable to the reaction parameter, ρ , obtained from the slopes of Hammett plots of other types of reactions.³² This calculation gives a ρ of 0.84 for the data in Figure 4B, indicating that the reduction of these compounds is slightly less sensitive to the substituent on the phenyl group than the acid dissociation of benzoic acid with a ρ value of 1.0. Hammett

plots for many aromatic redox couples give much larger ρ values, often > 2 .^{30–33} The modest value observed in our experiments is consistent with the substituents being located at some distance from the primary reduction site, the nitro group of the imidazole core.

Electrochemical Properties of 5-NI Alkenes under Aqueous Conditions

We conducted the initial electrochemical measurements in DMSO because the reduction of the 5-NIs is reversible under these conditions, as shown by the oxidation peak observed on the return scan in the CVs (Figure 4A). The resultant $E_{1/2}$ value (the potential midway between the two peak values) is close to the thermodynamic redox potential for reduction to the radical anion and thus provides a fundamental measure of the ease of adding the first electron to the different 5-NIs. While it is possible that the reduction of the 5-NIs occurs in a nonaqueous environment inside the microbial target cells (e.g., in the active site of a redox protein), it is likely that the reduction occurs in a more aqueous environment. Determination of the thermodynamic potential for reduction of 5-NIs in water is confounded by the fact that the electron transfers in aqueous conditions are irreversible reactions. This is shown by the lack of an oxidation peak on the return scan in the CVs in aqueous solution (Figure 4C). The irreversibility is due to the instability of the radical anion in aqueous solution, which upon protonation is further reduced at the same potential. Because of this, only the peak potential (E_p) for the reduction can be derived from the CVs (Table 6). In contrast to the $E_{1/2}$, the E_p is strongly affected by the kinetics of the electron transfer reactions and any coupled chemical reactions and may not be directly correlated with the thermodynamic redox potential for the overall reaction. Furthermore, the kinetic influence means that variations in the experimental conditions (e.g., differences in the electrode surface) will affect the E_p , possibly leading to greater scatter in the data.

For all of these reasons, we chose to rely on the $E_{1/2}$ values in DMSO rather than the aqueous E_p values as our primary indicator of the relative ease of reduction for the different 5-NIs. However, given that the first step in the reduction in aqueous solution at physiological pH is likely the same as that of the overall reaction in DMSO, i.e., one-electron reduction to the radical anion, we reasoned that the $E_{1/2}$ values in DMSO should give us an indication of the relative ease of reduction of the 5-NIs in aqueous solution. This is particularly likely among compounds of similar structure, for which the difference in solvation energy between DMSO and water would be expected to remain fairly constant across the series. In order to test this hypothesis, we determined the CVs of selected C2-olefinic 5-NI derivatives in neutral (pH 7.0) aqueous solution and correlated the data with the $E_{1/2}$ values obtained under anhydrous conditions (Table 6). A plot of E_p of the aqueous CVs vs $E_{1/2}$ for the same compounds in DMSO showed a strong linear correlation (Figure 4D), supporting the notion that the $E_{1/2}$ values obtained in DMSO give a reliable measure of the relative ease of reduction of the different 5-NIs independent of whether the reduction occurs in an aqueous or nonaqueous environment in the cell. It must be noted that the analysis of the true one-electron redox potential of the new 5-NI compounds in water would likely require other assay approaches, such as pulse radiolysis, although the utility of true aqueous one-electron potentials may be limited if reduction occurs in a purely aqueous environment in the cells conducive to rapid multielectron transfer.

Importance of Redox Potential of Modified 5-NI for Antimicrobial Potency and Selectivity

We next examined the relationship between $E_{1/2}$ and the ability to overcome Mz resistance (Figure 5A). In both pairs of Mz-sensitive and Mz-resistant *G. lamblia* lines, compounds with improved (i.e., decreased) resistance ratios generally had more positive $E_{1/2}$, although the importance of this relationship appeared to differ between the 713 and 106 pairs. In *G. lamblia* 713, almost all of the tested compounds showed some ability to overcome resistance, with the majority exhibiting more positive $E_{1/2}$ but a few compounds also showing more

negative $E_{1/2}$ (Figure 5A). By comparison, in *G. lamblia* 106, only compounds with more positive $E_{1/2}$ than Mz could overcome Mz resistance. This was not sufficient, however, since only about half of the compounds with more positive $E_{1/2}$ had a better (i.e., decreased) resistance ratio than Mz while the other half exhibited reduced anti-giardial activity compared to Mz in the Mz-resistant line (Figure 5A). Thus, a decrease in the energy requirements for redox activation, as reflected in a more positive $E_{1/2}$, is generally correlated with the ability of 5-NI to overcome Mz resistance, but such a decrease is neither necessary nor sufficient.

A similar conclusion also holds true for the overall anti-giardial activity of the nitro compounds, since we found a positive correlation between $E_{1/2}$ and activity (Figure 5B). However, several compounds (e.g., **20** and **27**) with more negative $E_{1/2}$ than Mz also exhibited increased anti-giardial activity compared to Mz, while others (e.g., **21** and **24**) had markedly more positive $E_{1/2}$ than Mz but only a very modest increase in activity (Tables 2, 3, 4, and 6). Rather surprisingly, comparison of $E_{1/2}$ and selectivity ratios revealed little correlation between these parameters (Figure 5C). Thus, many of the compounds with more negative $E_{1/2}$ than Mz showed low selectivity ratios, while compounds with markedly more positive $E_{1/2}$ had ratios comparable to or exceeding that of Mz. These results indicate that the ease of redox activation is not an important determinant of the selectivity of 5-NIs in *Giardia* compared to mammalian cells, at least as applied to the compounds tested in this study with their relatively limited $E_{1/2}$ range.

Conclusions

This study expands on prior work^{16,17} to demonstrate clearly that modification of the 2-position of the 5-NI core provides a promising avenue for improving its antimicrobial potency and selectivity. All of the new 5-NI derivatives were more potent than Mz against diverse isolates of *G. lamblia*, and almost a third (10 of 35) of these compounds showed 50- to 100-fold improvement in anti-giardial activity. Perhaps more importantly, a number of the new compounds markedly overcame resistance to Mz. With the current series of 5-NI derivatives and quantitative approaches, we did not identify compounds that could overcome Mz resistance completely, as no compound had identical activity against the Mz-resistant and Mz-sensitive pairs of isogenic *Giardia* lines. However, the quantitative analysis of anti-giardial activity revealed that the new compounds displayed a wide spectrum of activities in the face of Mz resistance, suggesting that a larger 5-NI library may well contain compounds whose activity is not compromised by prior Mz resistance.

Antimicrobial potency and ability to overcome Mz resistance were poorly if at all correlated. In fact, the compounds with the most improved Mz resistance ratios had only modest overall activity against the Mz-sensitive *G. lamblia* isolates, with pEC₅₀ values in the mid-range of those observed in the entire library. These results imply that the molecular properties that determine overall potency are not those that overcome Mz resistance, although detailed molecular conclusions are impossible to draw at present, given the lack of mechanistic insights into the relevant targets of 5-NIs in *G. lamblia*.

Analysis of the electrochemical properties of the new series of 5-NI compounds revealed fresh insights into the determinants of anti-giardial activity. Compounds with more positive redox activation potential, which makes them more readily reducible, generally had greater antimicrobial activity and an improved capacity to overcome Mz resistance. However, this relationship was not universal, as several compounds with more negative redox potentials also had markedly improved anti-giardial profiles, while other compounds with more positive redox potential did not. Thus, although easier redox activation can probably explain the improvement in anti-giardial activity profile for many of the compounds, it is neither necessary nor sufficient. Other yet to be defined molecular properties must therefore also be important. To our surprise,

we did not find a correlation between ease of redox activation and selectivity, as one might have expected from the general recognition that the excellent selectivity of 5-NI compounds for microbial targets over mammalian cells is based on the differences in the lowest redox couples present in these systems.¹¹ Our data suggest that, at least within the relatively negative and narrow $E_{1/2}$ range of compounds tested in this study, other determinants beyond ease of reduction affect toxicity and selectivity of 5-NIs, thus casting some doubts on the preeminence of the selective redox activation paradigm in explaining the clinical utility of 5-NI drugs.

The 5-NI compounds with a conjugated olefin bridge between the imidazole core and the pendant ring system generally had higher anti-giardial activity and better selectivity than those with a saturated alkane connection. In parallel, the energy requirements for nitro reduction were lower (i.e., more positive) in the conjugated compounds and were markedly impacted by the nature of the functional groups on the distant ring, whereas the same was not true in the alkanes. The most straightforward explanation may be that the olefin bridge allows effective electronic communication between the pendant ring system and the NI and thereby helps to fine-tune the nitro reducibility by distant functional groups. It needs to be borne in mind, however, that the electrochemical behavior of 5-NIs within the microbial target cells may be more complex than what can be modeled readily under cyclic voltammetry conditions in DMSO or water. Inside the target cells, the initial, rate-limiting reductive step presumably occurs in the presence of electrolytes, proteins, lipids, and other molecules with varying charges that may affect the charge distribution and, hence, reducibility and stability of the 5-NI radicals. In addition, the initial step is followed by a sequence of multielectron transfers, whose products may interact differently with microbial target molecules than the radical formed in the initial one-electron transfer reaction.³⁵

The study shows that 5-NI derivatives can be developed that are more potent than Mz in an animal model of giardiasis and have no apparent toxic side effects, making them good candidates for further preclinical development. The data caution, however, that in vivo activity can differ markedly from what might be expected on the basis of the observed in vitro activity. Such differences are most likely accounted for by differential pharmacokinetics of the respective compounds, which may be fruitful ground for future studies to develop the clinical potential of the new 5-NI compounds. Our results also stress that new compounds need to be tested rapidly in in vivo models to find truly effective drugs for treating giardiasis. In doing so, it should be possible to minimize the negative impact on development time and resource consumption that follows from the unavoidable attrition of compounds that are effective in vitro but exhibit poor in vivo activity.

Experimental Section

Chemistry

Materials and General Methods—Reagents and solvents were purchased from commercial sources and were used as received. Reaction progress was monitored by thin-layer chromatography on Merck silica gel 60 F-254 with detection by UV. Silica gel 60 (Merck 40–63 μm) was used for flash column chromatography. Melting points are uncorrected and were determined by use of a Thomas-Hoover Uni-Melt capillary melting point apparatus. ^1H NMR and ^{13}C NMR spectra were recorded with Bruker DRX-600, Bruker DRX-500, Varian 400, or Bruker AMX-400 spectrometers using $\text{DMSO}-d_6$ or CDCl_3 . Proton magnetic resonance (^1H NMR) spectra were recorded at 600, 500, or 400 MHz. Data are presented as follows: chemical shift (parts per million, ppm), multiplicity s = singlet, d = doublet, t = triplet, q = quartet, quin = quintet, sep = septet, m = multiplet, br = broad, coupling constant, J (in hertz), and integration. Carbon magnetic resonance (^{13}C NMR) spectra were recorded at 150, 125, or 100 MHz. Data for ^{13}C NMR are reported in terms of chemical shifts (ppm) and coupling constant J (in hertz) for fluorine-containing compounds. High-resolution mass spectra (HRMS) were recorded at

the mass spectrometry facility at The Scripps Research Institute, La Jolla, CA. Elemental analyses were performed by Midwest Microlab, LLC, Indianapolis, IN.

General Procedure for the Aldol Condensation—For the synthesis of 2-vinyl-5-nitroimidazoles by aldol condensation, dimetridazole (**4**, Table 1) was dissolved in EtOH (5.5 mL/mmol of dimetridazole) and treated with sodium ethoxide (NaOEt, 2.0–2.5 equiv). The resulting amber suspension was vigorously stirred at ambient temperature for 5–10 min before the addition of the aryl aldehydes (1.1–1.3 equiv) in small portions or dropwise using a syringe. The reaction mixture was then heated to 65 °C overnight, after which the brown reaction mixture was cooled to ambient temperature, transferred to a separatory funnel, and partitioned (CH₂Cl₂/H₂O). The organic phase was washed with brine (NaCl/H₂O), dried over anhydrous Na₂SO₄, and evaporated in vacuo to generally give a brown residue which was purified by column chromatography over silica gel.

1-Methyl-5-nitro-2-[(E)-2-phenylvinyl]-1H-imidazole (5)—Dimetridazole (5.0 g, 35.4 mmol) was reacted with benzaldehyde (4.5 g, 42.5 mmol, 1.2 equiv) in the presence of NaOEt (6.03 g, 88.6 mmol, 2.5 equiv). The mixture was purified by column chromatography (14% → 33% EtOAc/hexanes) to give **5** as a bright-yellow solid (1.6 g, 20%). ¹H NMR (500 MHz, CDCl₃) δ 8.10 (s, 1H), 7.89 (d, *J* = 15.8, 1H), 7.59–7.57 (m, 2H), 7.44–7.37 (m, 3H), 6.90 (d, *J* = 15.7, 1H), 4.06 (s, 3H); ¹³C NMR (125 MHz, CDCl₃) δ 149.8, 139.8, 135.2, 134.2, 129.8, 129.0, 127.5, 111.2, 32.8; HRMS (ESI⁺) calcd for C₁₂H₁₂N₃O₂ [M + H]⁺ 230.0924, found 230.0931. Anal. (C₁₂H₁₁N₃O₂) C, H, N.

1-Methyl-2-[(E)-2-(2-methylphenyl)vinyl]-5-nitro-1H-imidazole (6)—Dimetridazole (1.0 g, 7.1 mmol) was reacted with 2-methylbenzaldehyde (1.02 g, 8.5 mmol, 1.2 equiv) in the presence of NaOEt (1.2 g, 17.7 mmol, 2.5 equiv). The mixture was purified by column chromatography (85% CH₂Cl₂/hexanes → CH₂Cl₂). The material obtained in this manner was further purified by a recrystallization from CH₃OH (25 mL) to give **6** as a bright-yellow solid (0.40 g, 23%). ¹H NMR (400 MHz, CDCl₃) δ 8.15 (d, *J* = 15.6, 1H), 8.09 (s, 1H), 7.61 (dd, *J* = 7.2, 1.6, 1H), 7.30–7.22 (m, 3H), 6.81 (d, *J* = 15.6, 1H), 4.04 (s, 3H), 2.48 (s, 3H); ¹³C NMR (100 MHz, CDCl₃) δ 149.9, 137.4, 137.4, 137.3, 134.2, 134.1, 130.8, 129.5, 126.3, 125.5, 112.3, 32.7, 19.8; HRMS (ESI⁺) calcd for C₁₃H₁₄N₃O₂ [M + H]⁺ 244.1080, found 244.1076. Anal. (C₁₃H₁₃N₃O₂) C, H, N.

1-Methyl-2-[(E)-2-(3-methylphenyl)vinyl]-5-nitro-1H-imidazole (7)—Dimetridazole (3.5 g, 24.8 mmol) was reacted with 3-methylbenzaldehyde (3.53 mL, 29.8 mmol, 1.2 equiv) in the presence of NaOEt (4.2 g, 62 mmol, 2.5 equiv). The mixture was purified by column chromatography (CH₂Cl₂ → 10% CH₃OH/CH₂Cl₂) to give **7** as a yellow solid (2.53 g, 42%). ¹H NMR (400 MHz, CDCl₃) δ 8.04 (s, 1H), 7.80 (d, *J* = 15.6, 1H), 7.33 (s, 1H), 7.32 (d, *J* = 7.2, 1H), 7.27–7.21 (m, 1H), 7.14 (d, *J* = 7.6, 1H), 6.82 (d, *J* = 15.6, 1H), 3.99 (s, 3H), 2.34 (s, 3H); ¹³C NMR (100 MHz, CDCl₃) δ 149.9, 139.9, 138.6, 135.1, 134.2, 130.7, 128.8, 128.0, 124.7, 110.9, 32.7, 21.3; HRMS (ESI⁺) calcd for C₁₃H₁₄N₃O₂ [M + H]⁺ 244.1080, found 244.1083. Anal. (C₁₃H₁₃N₃O₂): C, 64.19; H, 5.39; N, 17.27. Found: C, 64.36; H, 5.50; N, 16.84.

1-Methyl-2-[(E)-2-(4-methylphenyl)vinyl]-5-nitro-1H-imidazole (8)—Dimetridazole (7.0 g, 49.6 mmol) was reacted with 4-methylbenzaldehyde (7.0 mL, 59.5 mmol, 1.2 equiv) in the presence of NaOEt (8.4 g, 124 mmol, 2.5 equiv). The mixture was purified by column chromatography (CH₂Cl₂ → 10% CH₃OH/CH₂Cl₂) to give **8** as a yellow solid (2.65 g, 22%). ¹H NMR (400 MHz, DMSO-*d*₆) δ 8.18 (s, 1H), 7.74 (d, *J* = 16.0, 1H), 7.68 (d, *J* = 8.0, 2H), 7.33 (d, *J* = 16.0, 1H), 7.24 (d, *J* = 8.0, 2H), 4.02 (s, 3H), 2.34 (s, 3H); ¹³C NMR (100 MHz, DMSO-*d*₆) δ 149.9, 139.2, 137.9, 134.2, 132.7, 129.4, 127.7, 127.4, 112.0, 32.7, 20.9;

HRMS (ESI⁺) calcd for C₁₃H₁₄N₃O₂ [M + H]⁺ 244.1080, found 244.1074. Anal. (C₁₃H₁₃N₃O₂): C, 64.19; H, 5.39; N, 17.27. Found: C, 64.32; H, 4.92; N, 16.85.

1-Methyl-2-[(E)-2-(2,4,6-trimethylphenyl)vinyl]-5-nitro-1H-imidazole (9)—

Dimetridazole (1.0 g, 7.1 mmol) was reacted with 2,4,6-trimethylbenzaldehyde (1.36 g, 9.23 mmol, 1.3 equiv) in the presence of NaOEt (966 mg, 14.2 mmol, 2.0 equiv). The mixture was purified by column chromatography (CH₂Cl₂ → 5% CH₃OH/CH₂Cl₂) to give **9** as a yellow solid (559 mg, 29%). ¹H NMR (400 MHz, CDCl₃) δ 8.10 (s, 1H), 7.97 (d, *J* = 16.0, 1H), 6.93 (s, 2H), 6.51 (d, *J* = 16.0, 1H), 3.99 (s, 3H), 2.39 (s, 6H), 2.30 (s, 3H); ¹³C NMR (100 MHz, CDCl₃) δ 149.8, 139.5, 138.1, 136.5, 134.0, 131.8, 129.9, 129.2, 116.5, 32.7, 21.2, 21.0; HRMS (ESI⁺) calcd for C₁₅H₁₈N₃O₂ [M + H]⁺ 272.1393, found 272.1397. Anal. (C₁₅H₁₇N₃O₂): C, 66.40; H, 6.32; N, 15.49. Found: C, 66.87; H, 6.40; N, 15.60.

2-[(E)-2-(2-Bromophenyl)vinyl]-1-methyl-5-nitro-1H-imidazole (10)—

Dimetridazole (1.0 g, 7.1 mmol) was reacted with 2-bromobenzaldehyde (1.6 g, 8.5 mmol, 1.2 equiv) in the presence of NaOEt (1.2 g, 17.7 mmol, 2.5 equiv). The mixture was purified by crystallization from CH₃OH/CH₂Cl₂ (1/1) to give **10** as a bright-yellow solid (0.44 g, 20%). ¹H NMR (600 MHz, CDCl₃) δ 8.22 (d, *J* = 15.7, 1H), 8.12 (s, 1H), 7.67 (dd, *J* = 7.9, 1.0, 1H), 7.65 (dd, *J* = 8.1, 0.8, 1H), 7.37 (t, *J* = 7.4, 1H), 7.24 (td, *J* = 7.7, 0.7, 1H), 6.87 (d, *J* = 15.6, 1H), 4.08 (s, 3H); ¹³C NMR (100 MHz, DMSO-*d*₆ + CD₂Cl₂) δ 149.2, 139.0, 135.6, 134.8, 133.8, 132.9, 130.6, 127.7, 127.6, 124.2, 115.6, 32.7; HRMS (ESI⁺) calcd for C₁₂H₁₁BrN₃O₂ [M + H]⁺ 308.0029, found 308.0034. Anal. (C₁₂H₁₀BrN₃O₂) C, H, N.

2-[(E)-2-(3-Bromophenyl)vinyl]-1-methyl-5-nitro-1H-imidazole (11)—

Dimetridazole (1.5 g, 10.6 mmol) was reacted with 3-bromobenzaldehyde (2.3 g, 12.7 mmol, 1.2 equiv) in the presence of NaOEt (1.8 g, 26.6 mmol, 2.5 equiv). The mixture was purified by column chromatography (20% EtOAc/hexanes) to give **11** as a bright-yellow solid (0.62 g, 19%). ¹H NMR (600 MHz, CDCl₃) δ 8.04 (s, 1H), 7.75 (d, *J* = 15.8, 1H), 7.52 (s, 1H), 7.47 (d, *J* = 7.7, 1H), 7.42 (d, *J* = 7.7, 2H), 6.88 (d, *J* = 15.7, 1H), 4.06 (s, 3H); ¹³C NMR (150 MHz, CDCl₃) δ 140.0, 143.1, 138.0, 133.8, 132.5, 130.4, 130.0, 129.7, 126.4, 125.2, 112.3, 32.8; HRMS (ESI⁺) calcd for C₁₂H₁₁BrN₃O₂ [M + H]⁺ 308.0029, found 308.0034. Anal. (C₁₂H₁₀BrN₃O₂): C, 46.78; H, 3.27; N, 13.64. Found: C, 47.65; H, 3.54; N, 13.08.

2-[(E)-2-(4-Bromophenyl)vinyl]-1-methyl-5-nitro-1H-imidazole (12)—

Dimetridazole (5.0 g, 35.4 mmol) was reacted with 4-bromobenzaldehyde (7.8 g, 42.5 mmol, 1.2 equiv) in the presence of NaOEt (6.0 g, 88.5 mmol, 2.5 equiv). The mixture was purified by column chromatography (CH₂Cl₂ → 10% CH₃OH/CH₂Cl₂) to give **12** as a yellow solid (7.8 g, 72%). ¹H NMR (400 MHz, DMSO-*d*₆) δ 8.06 (s, 1H), 7.81 (d, *J* = 16.0, 1H), 7.72 (d, *J* = 8.4, 2H), 7.61 (d, *J* = 8.4, 2H), 7.42 (d, *J* = 15.6, 1H), 4.13 (s, 3H); ¹³C NMR (100 MHz, DMSO-*d*₆) δ 149.4, 134.7, 134.0, 131.7, 130.8, 129.6, 128.4, 122.5, 114.0, 32.7; HRMS (ESI⁺) calcd for C₁₂H₁₁BrN₃O₂ [M + H]⁺ 308.0029, found 308.0026. Anal. (C₁₂H₁₀BrN₃O₂) C, H, N.

2-[(E)-2-(2-Chlorophenyl)vinyl]-1-methyl-5-nitro-1H-imidazole (13)—

Dimetridazole (1.0 g, 7.1 mmol) was reacted with 2-chlorobenzaldehyde (1.2 g, 8.5 mmol, 1.2 equiv) in the presence of NaOEt (1.2 g, 17.7 mmol, 2.5 equiv). The mixture was purified by crystallization from CH₃OH/CH₂Cl₂ (1/2) to give **13** as a bright-yellow solid (0.45 g, 24%). ¹H NMR (500 MHz, CDCl₃) δ 8.25 (d, *J* = 15.8, 1H), 8.12 (s, 1H), 7.69–7.67 (m, 1H), 7.46–7.43 (m, 1H), 7.34–7.30 (m, 2H), 6.92 (d, *J* = 15.7, 1H), 4.07 (s, 3H); ¹³C NMR (125 MHz, CDCl₃) δ 135.7, 134.6, 134.6, 134.9, 133.6, 130.5, 130.3, 127.1, 127.1, 114.1, 32.9; HRMS (ESI⁺) calcd for C₁₂H₁₁ClN₃O₂ [M + H]⁺ 264.0534, found 264.0539. Anal. (C₁₂H₁₀ClN₃O₂) C, H, N.

2-[(E)-2-(3-Chlorophenyl)vinyl]-1-methyl-5-nitro-1H-imidazole (14)—

Dimetridazole (1.0 g, 7.1 mmol) was reacted with 3-chlorobenzaldehyde (1.2 g, 8.5 mmol, 1.2 equiv) in the presence of NaOEt (1.2 g, 17.7 mmol, 2.5 equiv). The mixture was purified by crystallization from CH₃OH to give **14** as a bright-yellow solid (0.36 g, 19%). ¹H NMR (600 MHz, CDCl₃) δ 8.09 (s, 1H), δ 7.82 (d, *J* = 15.7, 1H), 7.57 (s, 1H), 7.43 (td, *J* = 4.6, 1.5, 1H), 7.36–7.35 (m, 2H), 6.90 (d, *J* = 15.7, 1H), 4.07 (s, 3H); ¹³C NMR (150 MHz, CDCl₃) δ 149.2, 139.1, 138.1, 137.0, 135.0, 134.1, 130.2, 129.6, 126.8, 126.0, 112.6, 32.8; HRMS (ESI⁺) calcd for C₁₂H₁₁ClN₃O₂ [M + H]⁺ 264.0534, found 264.0536. Anal. (C₁₂H₁₀ClN₃O₂) C, H, N.

2-[(E)-2-(4-Chlorophenyl)vinyl]-1-methyl-5-nitro-1H-imidazole (15)—

Dimetridazole (1.0 g, 7.1 mmol) was reacted with 4-chlorobenzaldehyde (1.2 g, 8.5 mmol, 1.2 equiv) in the presence of NaOEt (1.2 g, 17.7 mmol, 2.5 equiv). The mixture was purified by crystallization from CH₃OH/CH₂Cl₂ (3/1) to give **15** as a bright-yellow solid (0.27 g, 15%). ¹H NMR (500 MHz, CDCl₃) δ 8.10 (s, 1H), 7.85 (d, *J* = 15.7, 1H), 7.52 (d, *J* = 8.5, 2H), 7.40 (d, *J* = 8.5, 2H), 6.88 (d, *J* = 15.8, 1H), 4.07 (s, 3H); ¹³C NMR (125 MHz, CDCl₃) δ 149.5, 138.4, 135.7, 134.2, 133.7, 133.4, 129.3, 128.6, 111.7, 32.8; HRMS (ESI⁺) calcd for C₁₂H₁₁ClN₃O₂ [M + H]⁺ 264.0534, found 264.0535. Anal. (C₁₂H₁₀ClN₃O₂) C, H, N.

2-[(E)-2-(2,4-Dichlorophenyl)vinyl]-1-methyl-5-nitro-1H-imidazole (16)—

Dimetridazole (1.0 g, 7.1 mmol) was reacted with 2,4-dichlorobenzaldehyde (1.49 g, 9.23 mmol, 1.3 equiv) in the presence of NaOEt (966 mg, 14.2 mmol, 2.0 equiv). The mixture was purified by column chromatography (CH₂Cl₂ → 10% CH₃OH/CH₂Cl₂) to give **16** as a yellow solid (316 mg, 15%). ¹H NMR (DMSO-*d*₆) δ 8.20 (s, 1H), 8.19 (d, *J* = 8.8, 1H), 8.02 (d, *J* = 16.0, 1H), 7.73 (d, *J* = 2.0, 1H), 7.54 (d, *J* = 8.8, 1H), 7.53 (d, *J* = 16.0, 1H), 4.05 (s, 3H); ¹³C NMR (100 MHz, DMSO-*d*₆) δ 148.9, 134.3, 134.0, 133.7, 132.0, 131.0, 129.3, 129.2, 128.9, 127.8, 116.6, 32.8; HRMS (ESI⁺) calcd for C₁₂H₁₀Cl₂N₃O₂ [M + H]⁺ 298.0145, found 298.0135. Anal. (C₁₂H₉Cl₂N₃O₂): C, 48.34; H, 3.04; N, 14.09. Found: C, 48.50; H, 3.75; N, 13.87.

2-[(E)-2-(2-Iodophenyl)vinyl]-1-methyl-5-nitro-1H-imidazole (17)—Dimetridazole (1.0 g, 7.1 mmol) was reacted with 2-iodobenzaldehyde (2.0 g, 8.5 mmol, 1.2 equiv) in the presence of NaOEt (1.2 g, 17.7 mmol, 2.5 equiv). The mixture was purified by crystallization from CH₃OH/CH₂Cl₂ (1/2) to give **17** as a bright-orange solid (0.44 g, 20%). ¹H NMR (500 MHz, CDCl₃) δ 8.14 (s, 1H), 8.08 (d, *J* = 15.6, 1H), 7.94 (dd, *J* = 7.9, 1.2, 1H), 7.63 (dd, *J* = 7.9, 1.5, 1H), 7.41 (dt, *J* = 7.4, 0.6, 1H), 7.07 (dt, *J* = 7.7, 1.5, 1H), 6.79 (d, *J* = 15.5, 1H), 4.08 (s, 3H); ¹³C NMR (125 MHz, CDCl₃) δ 149.1, 143.1, 140.1, 138.7, 134.3, 130.8, 128.6, 126.8, 114.5, 100.9, 33.0; HRMS (ESI⁺) calcd for C₁₂H₁₁IN₃O₂ [M + H]⁺ 355.9891, found 355.9892. Anal. (C₁₂H₁₀IN₃O₂) C, H, N.

2-[(E)-2-(3-Iodophenyl)vinyl]-1-methyl-5-nitro-1H-imidazole (18)—Dimetridazole (1.0 g, 7.1 mmol) was reacted with 3-iodobenzaldehyde (2.0 g, 8.5 mmol, 1.2 equiv) in the presence of NaOEt (1.2 g, 17.7 mmol, 2.5 equiv). The mixture was purified by column chromatography (50% CH₂Cl₂/hexanes → 100% CH₂Cl₂) to give **18** as a dark-orange solid (0.50 g, 19%). ¹H NMR (600 MHz, CDCl₃) δ 8.09 (s, 1H), 7.93 (s, 1H), 7.77 (d, *J* = 15.7, 1H), 7.70 (d, *J* = 7.9, 1H), 7.50 (d, *J* = 7.74, 1H), 7.15 (t, *J* = 7.8, 1H), 6.87 (d, *J* = 15.7, 1H), 4.07 (s, 3H); ¹³C NMR (150 MHz, CDCl₃) δ 149.2, 139.1, 138.4, 137.8, 137.4, 135.7, 134.1, 130.6, 127.0, 124.5, 94.8, 32.8; HRMS (ESI⁺) calcd for C₁₂H₁₁IN₃O₂ [M + H]⁺ 355.9891, found 355.9902. Anal. (C₁₂H₁₀IN₃O₂): C, 40.58; H, 2.84; N, 11.83. Found: C, 41.07; H, 2.91; N, 11.12.

2-[(E)-2-(3-Fluorophenyl)vinyl]-1-methyl-5-nitro-1H-imidazole (19)—

Dimetridazole (1.0 g, 7.1 mmol) was reacted with 3-fluorobenzaldehyde (1.1 g, 8.5 mmol, 1.2

equiv) in the presence of NaOEt (1.2 g, 17.7 mmol, 2.5 equiv). The mixture was purified by column chromatography (50% CH₂Cl₂/hexanes → 100% CH₂Cl₂) to give **19** as a bright-yellow solid (0.23 g, 13%). ¹H NMR (500 MHz, CDCl₃) δ 8.10 (s, 1H), 7.86 (d, *J* = 15.7, 1H), 7.40–7.37 (m, 1H), 7.35–7.34 (m, 1H), 7.29 (dt, *J* = 10, 2.2, 1H), 7.09 (tdd, *J* = 8.1, 2.6, 1.0, 1H), 6.90 (d, *J* = 15.7, 1H), 4.08 (s, 3H); ¹³C NMR (150 MHz, CDCl₃) δ 163.1 (d, *J* = 245.2), 149.2, 139.1, 138.3 (d, *J* = 2.9), 137.5 (d, *J* = 7.3), 134.1, 130.5 (d, *J* = 8.1), 123.6 (d, *J* = 2.9), 116.6 (d, *J* = 21.5), 113.5 (d, *J* = 21.8), 112.5, 32.8; HRMS (ESI⁺) calcd for C₁₂H₁₁FN₃O₂ [M + H]⁺ 248.0830, found 248.0820. Anal. (C₁₂H₁₀FN₃O₂) C, H, N.

2-[(*E*)-2-(3-Methoxyphenyl)vinyl]-1-methyl-5-nitro-1*H*-imidazole (**20**)—

Dimetridazole (1.0 g, 7.1 mmol) was reacted with 3-methoxybenzaldehyde (1.13 mL, 9.23 mmol, 1.3 equiv) in the presence of NaOEt (966 mg, 14.2 mmol, 2.0 equiv). The mixture was purified by column chromatography (CH₂Cl₂ → 5% CH₃OH/CH₂Cl₂) to give **20** as a yellow solid (588 mg, 32%). ¹H NMR (400 MHz, DMSO-*d*₆) δ 8.14 (s, 1H), 7.70 (d, *J* = 16.0, 1H), 7.35 (d, *J* = 16.0, 1H), 7.34 (br s, 1H), 7.29 (d, *J* = 5.2, 1H), 6.93–6.90 (m, 1H), 3.99 (s, 3H), 3.77 (s, 3H); ¹³C NMR (100 MHz, DMSO-*d*₆) δ 159.6, 149.7, 139.0, 137.9, 136.8, 134.1, 129.8, 120.5, 115.3, 113.3, 112.4, 55.2, 32.8; HRMS (ESI⁺) calcd for C₁₃H₁₄N₃O₃ [M+H]⁺ 260.1030, found 260.1029. Anal. (C₁₃H₁₃N₃O₃) C, H, N.

1-Methyl-5-nitro-2-[(*E*)-2-[4-(trifluoromethoxy)phenyl]vinyl]-1*H*-imidazole (**21**)—

Dimetridazole (1.0 g, 7.1 mmol) was reacted with 4-(trifluoromethoxy)benzaldehyde (1.33 mL, 9.23 mmol, 1.3 equiv) in the presence of NaOEt (966 mg, 14.2 mmol, 2.0 equiv). The mixture was purified by column chromatography (CH₂Cl₂ → 10% CH₃OH/CH₂Cl₂) to give **21** as a yellow solid (311 mg, 14%). ¹H NMR (400 MHz, DMSO-*d*₆) δ 8.13 (s, 1H), 7.88 (d, *J* = 8.8, 2H), 7.73 (d, *J* = 15.6, 1H), 7.38 (d, *J* = 15.6, 2H), 7.36 (d, *J* = 8.8, 1H), 3.98 (s, 3H); ¹³C NMR (100 MHz, DMSO-*d*₆) δ 149.3, 148.6, 148.5, 148.6, 148.6, 142.0, 139.1, 136.1, 134.8, 134.0, 129.5, 128.0, 121.2, 120.6, 118.7, 114.3, 32.8; HRMS (ESI⁺) calcd for C₁₃H₁₁F₃N₃O₃ [M + H]⁺ 314.0747, found 314.0752. Anal. (C₁₃H₁₀F₃N₃O₃): C, 49.85; H, 3.22; N, 13.42. Found: C, 49.92; H, 3.60; N, 13.88.

1-Methyl-5-nitro-2-[(*E*)-2-(2,3,4-trimethoxyphenyl)vinyl]-1*H*-imidazole (**22**)—

Dimetridazole (1.0 g, 7.1 mmol) was reacted with 2,3,4-trimethoxybenzaldehyde (1.67 g, 8.52 mmol, 1.2 equiv) in the presence of NaOEt (1.2 g, 17.8 mmol, 2.5 equiv). The mixture was purified by column chromatography (CH₂Cl₂ → 10% CH₃OH/CH₂Cl₂) to give **22** as a yellow solid (362 mg, 16%). ¹H NMR (400 MHz, CDCl₃) δ 8.06 (s, 1H), 7.94 (d, *J* = 16.0, 1H), 7.23 (d, *J* = 8.8, 1H), 6.96 (d, *J* = 16.0, 1H), 6.68 (d, *J* = 8.8, 1H), 4.00 (s, 3H), 3.93 (s, 3H), 3.88 (s, 3H), 3.87 (s, 3H); ¹³C NMR (100 MHz, CDCl₃) δ 155.1, 152.9, 150.7, 142.4, 138.7, 135.2, 134.4, 123.4, 122.2, 110.6, 107.5, 61.1, 60.8, 56.0, 32.6; HRMS (ESI⁺) calcd for C₁₅H₁₈N₃O₅ [M + H]⁺ 320.1241, found 320.1240. Anal. (C₁₅H₁₇N₃O₅) C, H, N.

2-[(*E*)-2-[4-(Diethoxymethyl)phenyl]vinyl]-1-methyl-5-nitro-1*H*-imidazole (**23**)—

Dimetridazole (20 g, 142 mmol) was reacted with 4-(diethoxymethyl)benzaldehyde (34.5 mL, 170 mmol, 1.2 equiv) in the presence of NaOEt (24 g, 354 mmol, 2.5 equiv). The mixture was purified by column chromatography (CH₂Cl₂ → 10% CH₃OH/CH₂Cl₂) to give **23** as a yellow solid (5.67 g, 24%). ¹H NMR (400 MHz, CDCl₃) δ 8.09 (s, 1H), 7.87 (d, *J* = 16.0, 1H), 7.56 (d, *J* = 8.0, 2H), 7.51 (d, *J* = 8.0, 2H), 6.89 (d, *J* = 16.0, 1H), 5.52 (s, 1H), 4.05 (s, 3H), 3.65–3.53 (m, 4H, 2 × OCH₂CH₃), 1.25 (t, *J* = 7.2, 6H, 2 × OCH₂CH₃); ¹³C NMR (100 MHz, CDCl₃) δ 149.8, 140.9, 139.4, 135.2, 134.2, 127.3, 111.3, 101.0, 89.8, 61.1, 32.8, 15.2; HRMS (ESI⁺) calcd for C₁₇H₂₂N₃O₄ [M + H]⁺ 332.1605, found 332.1608. Anal. (C₁₇H₂₁N₃O₄) C, H, N.

2-[(E)-2-Biphenyl-2-ylvinyl]-1-methyl-5-nitro-1H-imidazole (24)—Dimetridazole (1.0 g, 7.1 mmol) was reacted with biphenyl-2-carbaldehyde (1.67 g, 9.23 mmol, 1.3 equiv) in the presence of NaOEt (966 mg, 14.2 mmol, 2.0 equiv). The mixture was purified by column chromatography (CH₂Cl₂ → 5% CH₃OH/CH₂Cl₂) to give **24** as a yellow solid (455 mg, 21%). ¹H NMR (400 MHz, DMSO-*d*₆) δ 8.13–8.12 (m, 1H), 8.08 (s, 1H), 7.70 (d, *J* = 15.6, 1H), 7.51–7.43 (m, 5H), 7.39–7.32 (m, 4H), 4.02 (s, 3H); ¹³C NMR (100 MHz, CDCl₃) δ 149.7, 141.7, 139.8, 138.9, 135.9, 134.0, 132.9, 130.3, 129.5, 129.2, 128.3, 127.7, 127.4, 126.5, 113.7, 32.7; HRMS (ESI⁺) calcd for C₁₈H₁₆N₃O₂ [M + H]⁺ 306.1237, found 306.1225. Anal. (C₁₈H₁₅N₃O₂) C, H, N.

1-Methyl-2-[(E)-2-(1-naphthyl)vinyl]-5-nitro-1H-imidazole (25)—Dimetridazole (1.0 g, 7.1 mmol) was reacted with 1-naphthaldehyde (1.25 mL, 9.23 mmol, 1.3 equiv) in the presence of NaOEt (966 mg, 14.2 mmol, 2.0 equiv). The mixture was purified by column chromatography (CH₂Cl₂ → 10% CH₃OH/CH₂Cl₂) to give **25** as a yellow solid (554 mg, 28%). ¹H NMR (400 MHz, DMSO-*d*₆) δ 8.59 (d, *J* = 15.6, 1H), 8.26 (d, *J* = 8.4, 1H), 8.25 (s, 1H), 8.16 (d, *J* = 8.0, 1H), 8.01–7.99 (m, 2H), 7.66–7.59 (m, 3H), 7.49 (d, *J* = 15.6, 1H), 4.08 (s, 3H); ¹³C NMR (100 MHz, CDCl₃) δ 149.7, 134.1, 133.7, 133.3, 132.0, 130.6, 129.7, 128.7, 127.0, 126.1, 125.8, 125.6, 124.6, 128.8, 115.5, 32.8; HRMS (ESI⁺) calcd for C₁₆H₁₄N₃O₂ [M + H]⁺ 280.1080, found 280.1085. Anal. (C₁₆H₁₃N₃O₂) C, H, N.

1-Methyl-2-[(E)-2-(2-naphthyl)vinyl]-5-nitro-1H-imidazole (26)—Dimetridazole (1.0 g, 7.1 mmol) was reacted with 2-naphthaldehyde (1.44 g, 9.23 mmol, 1.3 equiv) in the presence of NaOEt (966 mg, 14.2 mmol, 2.0 equiv). The mixture was purified by column chromatography (CH₂Cl₂ → 10% CH₃OH/CH₂Cl₂) to give **26** as a yellow solid (385 mg, 19%). ¹H NMR (400 MHz, DMSO-*d*₆) δ 8.22 (s, 1H), 8.21 (br s, 1H), 8.07 (dd, *J* = 8.8, 1.6, 1H), 7.98–7.92 (m, 4H), 7.56–7.52 (m, 3H), 4.08 (s, 3H); ¹³C NMR (100 MHz, CDCl₃) δ 149.8, 137.8, 134.2, 133.3, 133.1, 133.0, 128.6, 128.3, 128.2, 127.6, 126.9, 126.8, 126.6, 123.9, 113.5, 32.8; HRMS (ESI⁺) calcd for C₁₆H₁₄N₃O₂ [M + H]⁺ 280.1080, found 280.1081. Anal. (C₁₆H₁₃N₃O₂): C, 68.81; H, 4.69; N, 15.05. Found: C, 68.21; H, 4.78; N, 14.95.

2-[(E)-2-(3a,7a-Dihydro-1,3-benzodioxol-5-yl)vinyl]-1-methyl-5-nitro-1H-imidazole (27)—Dimetridazole (1.0 g, 7.1 mmol) was reacted with piperonal (1.39 g, 9.23 mmol, 1.3 equiv) in the presence of NaOEt (966 mg, 14.2 mmol, 2.0 equiv). The mixture was purified by column chromatography (CH₂Cl₂ → 10% CH₃OH/CH₂Cl₂) to give **27** as a yellow solid (600 mg, 31%). ¹H NMR (400 MHz, DMSO-*d*₆) δ 8.17 (s, 1H), 7.70 (d, *J* = 15.6, 1H), 7.57 (d, *J* = 1.6, 1H), 7.25 (d, *J* = 15.6, 1H), 7.21 (dd, *J* = 8.0, 1.6, 1H), 6.96 (d, *J* = 8.0, 1H), 6.09 (s, 2H), 4.01 (s, 3H); ¹³C NMR (100 MHz, CDCl₃) δ 150.1, 148.4, 148.0, 137.9, 134.3, 130.0, 124.0, 111.0, 108.4, 106.0, 101.4, 89.3, 32.7; HRMS (ESI⁺) calcd for C₁₃H₁₂N₃O₄ [M + H]⁺ 274.0822, found 274.0823. Anal. (C₁₃H₁₁N₃O₄) C, H, N.

1-Methyl-2-[(E)-2-(1-methyl-1H-imidazol-2-yl)vinyl]-5-nitro-1H-imidazole (28)—Dimetridazole (1.06 g, 7.5 mmol) was reacted with 1-methyl-1H-imidazole-2-carbaldehyde (1.0 g, 9.1 mmol, 1.2 equiv) in the presence of NaOEt (1.27 g, 18.8 mmol, 2.5 equiv). The mixture was purified by column chromatography (CH₂Cl₂ → 10% CH₃OH/CH₂Cl₂) to give **28** as a yellow solid (1.36 g, 77%). ¹H NMR (400 MHz, DMSO-*d*₆) δ 8.20 (s, 1H), 7.64 (d, *J* = 15.2, 1H), 7.33 (d, *J* = 15.2, 1H), 7.31 (s, 1H), 7.07 (s, 1H), 3.99 (s, 3H), 3.78 (s, 3H); ¹³C NMR (100 MHz, CDCl₃) δ 149.3, 143.4, 134.1, 129.2, 124.0, 123.0, 113.6, 32.7, 32.4; HRMS (ESI⁺) calcd for C₁₀H₁₂N₅O₂ [M + H]⁺ 234.0985, found 234.0986. Anal. (C₁₀H₁₁N₅O₂) C, H, N.

2-[(E)-2-(2-Furyl)vinyl]-1-methyl-5-nitro-1H-imidazole (29)—Dimetridazole (1.0 g, 7.1 mmol) was reacted with furan-2-carbaldehyde (0.65 mL, 7.81 mmol, 1.1 equiv) in the

presence of NaOEt (1.2 g, 17.8 mmol, 2.5 equiv). The mixture was purified by column chromatography ($\text{CH}_2\text{Cl}_2 \rightarrow 10\% \text{CH}_3\text{OH}/\text{CH}_2\text{Cl}_2$) to give **29** as a yellow solid (825 mg, 53%). ^1H NMR (400 MHz, $\text{DMSO}-d_6$) δ 8.18 (s, 1H), 7.83 (d, $J = 1.6$, 1H), 7.58 (d, $J = 15.6$, 1H), 7.00 (d, $J = 15.6$, 1H), 6.90 (d, $J = 3.2$, 1H), 6.64 (dd, $J = 3.2, 2.0$, 1H), 3.98 (s, 3H); ^{13}C NMR (100 MHz, CDCl_3) δ 151.4, 149.5, 144.9, 139.0, 134.2, 124.8, 113.6, 112.7, 110.3, 32.6; HRMS (ESI^+) calcd for $\text{C}_{10}\text{H}_{10}\text{N}_3\text{O}_3$ [$\text{M} + \text{H}$] $^+$ 220.0717, found 220.0720. Anal. ($\text{C}_{10}\text{H}_9\text{N}_3\text{O}_3$) C, H, N.

1-Methyl-5-nitro-2-[(E)-2-(2-thienyl)vinyl]-1H-imidazole (30)—Dimetridazole (1.0 g, 7.1 mmol) was reacted with thiophene-2-carbaldehyde (0.86 mL, 9.23 mmol, 1.3 equiv) in the presence of NaOEt (966 mg, 14.2 mmol, 2.0 equiv). The mixture was purified by column chromatography ($\text{CH}_2\text{Cl}_2 \rightarrow 10\% \text{CH}_3\text{OH}/\text{CH}_2\text{Cl}_2$) to give **30** as a yellow solid (384 mg, 23%). ^1H NMR (400 MHz, $\text{DMSO}-d_6$) δ 8.18 (s, 1H), 7.90 (d, $J = 1.6$, 1H), 7.78 (d, $J = 15.6$, 1H), 7.70 (dd, $J = 5.2, 1.2$, 1H), 7.63 (dd, $J = 4.8, 2.8$, 1H), 7.21 (d, $J = 15.6$, 1H), 4.00 (s, 3H); ^{13}C NMR (100 MHz, CDCl_3) δ 150.0, 138.9, 138.7, 134.2, 132.1, 127.4, 125.6, 112.6, 32.7; HRMS (ESI^+) calcd for $\text{C}_{10}\text{H}_{10}\text{N}_3\text{O}_2\text{S}$ [$\text{M} + \text{H}$] $^+$ 236.0488, found 236.0491. Anal. ($\text{C}_{10}\text{H}_9\text{N}_3\text{O}_2\text{S}$): C, 51.05; H, 3.86; N, 17.86. Found: C, 51.48; H, 3.35; N, 17.57.

1-Methyl-5-nitro-2-[(E)-2-(3-thienyl)vinyl]-1H-imidazole (31)—Dimetridazole (1.0 g, 7.1 mmol) was reacted with thiophene-3-carbaldehyde (0.81 mL, 9.23 mmol, 1.3 equiv) in the presence of NaOEt (966 mg, 14.2 mmol, 2.0 equiv). The mixture was purified by column chromatography ($\text{CH}_2\text{Cl}_2 \rightarrow 10\% \text{CH}_3\text{OH}/\text{CH}_2\text{Cl}_2$) to give **31** as a yellow solid (367 mg, 22%). ^1H NMR (400 MHz, $\text{DMSO}-d_6$) δ 8.18 (s, 1H), 7.91 (d, 15.6, 1H), 7.67 (d, $J = 5.2$, 1H), 7.52 (d, $J = 3.6$, 1H), 7.15 (dd, $J = 5.2, 3.6$, 1H), 7.03 (d, $J = 15.6$, 1H), 3.99 (s, 3H); ^{13}C NMR (100 MHz, CDCl_3) δ 149.5, 140.3, 138.9, 134.2, 130.8, 130.1, 128.5, 128.3, 111.6, 32.7; HRMS (ESI^+) calcd for $\text{C}_{10}\text{H}_{10}\text{N}_3\text{O}_2\text{S}$ [$\text{M} + \text{H}$] $^+$ 236.0488, found 236.0493. Anal. ($\text{C}_{10}\text{H}_9\text{N}_3\text{O}_2\text{S}$): C, 51.05; H, 3.86; N, 17.86. Found: C, 50.90; H, 3.54; N, 17.67.

2-[1,2-Dibromo-2-(4-bromophenyl)ethyl]-1-methyl-5-nitro-1H-imidazole (33)—Compound **12** (2.05 g, 6.7 mmol) was dissolved in anhydrous CHCl_3 (120 mL), and the pale-yellow solution was cooled to 0 °C. Bromine (0.37 mL, 1.12 g, 7.03 mmol, 1.05 equiv) was added via syringe at 0 °C, and the resulting orange solution was stirred at ambient temperature for 4 h. The mixture was transferred to a separatory funnel and partitioned ($\text{CH}_2\text{Cl}_2/\text{H}_2\text{O}$). The organic phase was washed with $\text{Na}_2\text{S}_2\text{O}_3$ (3 \times 100 mL), brine ($\text{NaCl}/\text{H}_2\text{O}$, 2 \times 50 mL), dried over Na_2SO_4 , and evaporated in vacuo to give a pale-yellow solid. The residue was purified by column chromatography (hexanes \rightarrow 30% EtOAc/hexanes) to give **33** as an off-white solid (2.73 g, 88%). ^1H NMR (400 MHz, $\text{DMSO}-d_6$) δ 8.20 (s, 1H), 7.74 (d, $J = 8.4$, 2H), 7.61 (d, $J = 8.4$, 2H), 6.49 (d, $J = 11.2$, 1H), 6.03 (d, $J = 11.6$, 1H), 4.01 (s, 3H); ^{13}C NMR (100 MHz, CDCl_3) δ 149.1, 139.1, 138.4, 132.3, 131.5, 130.7, 122.3, 51.7, 42.0, 33.3; HRMS (ESI^+) calcd for $\text{C}_{12}\text{H}_{11}\text{Br}_3\text{N}_3\text{O}_2$ [$\text{M} + \text{H}$] $^+$ 465.8296, found 465.8394. Anal. ($\text{C}_{12}\text{H}_{10}\text{Br}_3\text{N}_3\text{O}_2$) C, H, N.

1-(1-Methyl-5-nitro-1H-imidazol-2-yl)-2-(4-methylphenyl)ethane-1,2-diol (34)—Compound **8** (0.69 g, 2.85 mmol) was made into a suspension in *t*-BuOH/ H_2O (1:1, 37 mL). Citric acid (1.10 g, 5.7 mmol, 2.0 equiv) was added in one portion followed by potassium osmate dihydrate (2.1 mg, 0.0057 mmol, 0.2 mol %). To the black suspension was added *N*-methylmorpholine *N*-oxide (NMO, 0.32 mL, 1.1 equiv) dropwise at ambient temperature, and the resulting suspension was stirred vigorously overnight. The mixture was filtered through Celite, and the brown filtrate was transferred to a separatory funnel and partitioned ($\text{CH}_2\text{Cl}_2/\text{H}_2\text{O}$). The organic phase was washed with brine (2 \times 100 mL), dried over Na_2SO_4 , and evaporated in vacuo to give a brown residue. Crude product was purified by column chromatography (EtOAc) to give **34** as a yellowish solid (220 mg, 28%). ^1H NMR (400 MHz,

$\text{CDCl}_3 + \text{CD}_3\text{OD}$) δ 7.86 (s, 1H), 7.01 (s, 4H), 4.92 (d, $J = 6.9$, 1H), 4.64 (d, $J = 6.9$, 1H), 3.49 (s, 3H), 3.35 (br s, 2H), 2.23 (s, 3H); ^{13}C NMR (100 MHz, $\text{CDCl}_3 + \text{CD}_3\text{OD}$) δ 151.4, 138.0, 135.8, 131.3, 129.0, 129.0, 126.2, 75.6, 70.9, 32.8, 20.9; HRMS (ESI⁺) calcd for $\text{C}_{13}\text{H}_{16}\text{N}_3\text{O}_4$ [$\text{M} + \text{H}$]⁺ 278.1135, found 278.1137. Anal. ($\text{C}_{13}\text{H}_{15}\text{N}_3\text{O}_4$): C, 56.31; H, 5.45; N, 15.15. Found: C, 56.41; H, 5.44; N, 15.11.

1-(4-Bromophenyl)-2-(1-methyl-5-nitro-1*H*-imidazol-2-yl)-ethane-1,2-diol (35)—Compound **12** (1.42 g, 4.62 mmol) was made into a suspension in 1:1 *t*-BuOH/ H_2O (60 mL). Citric acid (1.78 g, 9.25 mmol, 2.0 equiv) was added in one portion followed by potassium osmate dihydrate (3.0 mg, 0.0092 mmol, 0.2 mol %). To the black suspension was added *N*-methylmorpholine *N*-oxide (NMO, 0.52 mL, 5.08 mmol, 1.1 equiv) dropwise at ambient temperature, and the resulting suspension was stirred vigorously overnight. The mixture was filtered through Celite, and the brown filtrate was transferred to a separatory funnel and partitioned ($\text{CH}_2\text{Cl}_2/\text{H}_2\text{O}$). The organic phase was washed with brine (2 \times 100 mL), dried over Na_2SO_4 , and evaporated in vacuo to give a brown residue. The residue was purified by column chromatography ($\text{CH}_2\text{Cl}_2 \rightarrow$ 5% MeOH/ CH_2Cl_2) to give diol **35** as a white foam (225 mg, 14%). ^1H NMR (400 MHz, $\text{DMSO}-d_6$) δ 7.96 (s, 1H), 7.43 (d, $J = 8.4$, 2H), 7.21 (d, $J = 8.4$, 2H), 6.07 (d, $J = 4.8$, 1H), 5.81 (d, $J = 4.8$, 1H), 4.93–4.91 (m, 1H), 4.80–4.78 (m, 1H), 3.85 (s, 3H); ^{13}C NMR (100 MHz, CDCl_3) δ 152.1, 140.9, 138.9, 131.6, 130.5, 129.1, 120.2, 74.1, 71.5, 33.4; HRMS (ESI⁺) calcd for $\text{C}_{12}\text{H}_{13}\text{BrN}_3\text{O}_4$ [$\text{M} + \text{H}$]⁺ 342.0084, found 342.0086. Anal. ($\text{C}_{12}\text{H}_{12}\text{BrN}_3\text{O}_4$): C, 42.12; H, 3.54; N, 12.28. Found: C, 41.84; H, 3.77; N, 12.47.

1-(1-Methyl-5-nitro-1*H*-imidazol-2-yl)-2-(4-methylphenyl)-ethane-1,2-diyl Diacetate (36)—Diol **34** (90 mg, 0.325 mmol) was dissolved in anhydrous pyridine (0.5 mL), and the solution was cooled to 0 °C. Acetic anhydride (132.6 mg, 122 μL , 1.3 mmol, 4.0 equiv) was added dropwise via syringe, and the resulting solution was stirred at ambient temperature for 3 h. The mixture was transferred to a separatory funnel and partitioned ($\text{CH}_2\text{Cl}_2/\text{H}_2\text{O}$). The organic phase was washed with 1.0 N HCl (2 \times 50 mL), brine (2 \times 50 mL), dried over Na_2SO_4 , and evaporated in vacuo to give a yellow oil. The residue was purified by column chromatography (hexanes \rightarrow 40% EtOAc/hexanes) to provide acetylated adduct **36** as a yellowish wax (74 mg, 66%). ^1H NMR (400 MHz, CDCl_3) δ 7.93 (s, 1H), 7.11–7.04 (m, 4H), 6.36 (d, $J = 9.4$, 1H), 5.93 (d, $J = 9.4$, 1H), 3.62 (s, 3H), 2.28 (s, 3H), 2.13 (s, 3H), 2.11 (s, 3H); ^{13}C NMR (100 MHz, CDCl_3) δ 170.4, 169.2, 147.0, 139.3, 138.5, 132.5, 131.7, 129.4, 127.0, 74.7, 68.6, 32.7, 21.6, 21.0, 20.6; HRMS (ESI⁺) calcd for $\text{C}_{17}\text{H}_{19}\text{N}_3\text{O}_6\text{Na}$ [$\text{M} + \text{Na}$]⁺ 384.1166, found 384.1172. Anal. ($\text{C}_{17}\text{H}_{19}\text{N}_3\text{O}_6$): C, 56.51; H, 5.30; N, 11.63. Found: C, 53.32; H, 5.13; N, 10.22.

1-(1-Methyl-5-nitro-1*H*-imidazol-2-yl)-2-(4-bromophenyl)-ethane-1,2-diyl Diacetate (37)—Diol **35** (200 mg, 0.58 mmol) was dissolved in anhydrous pyridine (10 mL), and the solution was cooled to 0 °C. Acetic anhydride (0.14 mL, 1.45 mmol, 2.5 equiv) was added dropwise via syringe, and the resulting solution was stirred at ambient temperature for 3 h. The mixture was transferred to a separatory funnel and partitioned ($\text{CH}_2\text{Cl}_2/\text{H}_2\text{O}$). The organic phase was washed with 1.0 N HCl (2 \times 50 mL), brine (2 \times 50 mL), dried over Na_2SO_4 , and evaporated in vacuo to give a yellow oil. The residue was purified by column chromatography (hexanes \rightarrow 40% EtOAc/hexanes) to provide acetylated adduct **37** as a colorless oil (227 mg, 92%). ^1H NMR (400 MHz, CDCl_3) δ 7.93 (s, 1H), 7.41 (d, $J = 8.4$, 2H), 7.13 (d, $J = 8.4$, 2H), 6.39 (d, $J = 9.2$, 1H), 5.96 (d, $J = 9.2$, 1H), 3.73 (s, 3H), 2.13 (s, 3H), 2.11 (s, 3H); ^{13}C NMR (100 MHz, CDCl_3) δ 170.3, 169.1, 146.4, 143.9, 133.9, 132.4, 132.0, 129.0, 123.5, 74.1, 68.0, 32.9, 20.9, 20.6; HRMS (ESI⁺) calcd for $\text{C}_{16}\text{H}_{17}\text{BrN}_3\text{O}_6$ [$\text{M} + \text{H}$]⁺ 426.0295, found 426.0300. Anal. ($\text{C}_{16}\text{H}_{16}\text{BrN}_3\text{O}_6$) C, H, N.

1-Methyl-5-nitro-2-(2-phenylethyl)-1H-imidazole (40)—Compound **5** (1.0 g, 4.37 mmol), *p*-toluenesulfonylhydrazine (4.06 g, 21.82 mmol, 5.0 equiv), and K₂CO₃ (3.02 g, 21.82 mmol, 5.0 equiv) in pyridine (30 mL) were stirred at 120 °C for 14 h. Purification of the mixture was carried out by preparatory thin layer chromatography on silica gel, eluting with 70% EtOAc/hexanes to furnish **40** as a white solid (0.324 g, 32%). ¹H NMR (600 MHz, CDCl₃) δ 8.00 (s, 1H), 7.35–7.29 (m, 2H), 7.25 (tt, *J* = 7.2, 1.7, 1H), 7.14 (dd, *J* = 7.0, 1.3, 2H), 3.26 (s, 3H), 3.13 (t, *J* = 7.3, 2H), 3.04 (t, *J* = 8.0, 2H); ¹³C NMR (150 MHz, CDCl₃) δ 152.6, 139.8, 138.8, 132.6, 128.8, 128.3, 126.8, 33.6, 32.7, 29.7; HRMS (ESI⁺) calcd for C₁₂H₁₄N₃O₂ [M + H]⁺ 232.1080, found 232.1083. Anal. (C₁₂H₁₃N₃O₂): C, 62.33; H, 5.67; N, 18.17. Found: C, 62.71; H, 5.77; N, 17.57.

1-Methyl-2-[2-(4-methylphenyl)ethyl]-5-nitro-1H-imidazole (41)—Compound **8** (0.9 g, 3.75 mmol), *p*-toluenesulfonylhydrazine (3.49 g, 18.8 mmol, 5.0 equiv), and K₂CO₃ (2.59 g, 18.8 mmol, 5.0 equiv) in anhydrous pyridine (30 mL) were stirred at 120 °C for 14 h. The mixture was cooled to ambient temperature, transferred to a separatory funnel, and partitioned (CH₂Cl₂/H₂O). The organic phase was washed with brine (NaCl/H₂O, 2 × 50 mL), NaHCO₃/H₂O (2 × 50 mL), dried over Na₂SO₄, and evaporated in vacuo to give a brown residue. The residue was purified by flash chromatography (CH₂Cl₂ → 5% MeOH/CH₂Cl₂) to give **41** as a pale-yellow solid (166 mg, 18%). ¹H NMR (400 MHz, CDCl₃) δ 7.98 (s, 1H), 7.10 (d, *J* = 8.0, 2H), 7.03 (d, *J* = 8.0, 2H), 3.66 (s, 3H), 3.10–3.06 (m, 2H), 3.04–2.99 (m, 2H), 2.33 (s, 3H); ¹³C NMR (100 MHz, CDCl₃) δ 152.7, 136.6, 136.2, 132.5, 129.3, 128.1, 127.9, 33.0, 32.7, 29.6, 20.9; HRMS (ESI⁺) calcd for C₁₃H₁₆N₃O₂ [M + H]⁺ 246.1237, found 246.1239. Anal. (C₁₃H₁₅N₃O₂): C, 63.66; H, 6.16; N, 17.13. Found: C, 63.15; H, 6.54; N, 17.65.

2-[2-(4-Bromophenyl)ethyl]-1-methyl-5-nitro-1H-imidazole (42)—Compound **12** (0.9 g, 2.95 mmol), *p*-toluenesulfonylhydrazine (2.73 g, 14.7 mmol, 5.0 equiv), and K₂CO₃ (2.03 g, 14.7 mmol, 5.0 equiv) in anhydrous pyridine (30 mL) were stirred at 120 °C for 14 h. The mixture was transferred to a separatory funnel and partitioned (CH₂Cl₂/H₂O). The organic phase was washed with 1.0 N HCl (3 × 100 mL), dried over Na₂SO₄, and evaporated in vacuo to give a brown residue which was purified by flash chromatography (hexanes → 40% EtOAc/hexanes) to provide **42** as an off-white solid (151 mg, 17%). ¹H NMR (400 MHz, DMSO-*d*₆) δ 8.03 (s, 1H), 7.47 (d, *J* = 8.4, 2H), 7.23 (d, *J* = 8.4, 2H), 3.78 (s, 3H), 3.07–3.04 (m, 2H), 3.03–2.98 (m, 2H); ¹³C NMR (100 MHz, CDCl₃) δ 152.8, 139.8, 138.7, 132.2, 131.0, 130.7, 119.1, 32.7, 31.3, 28.0; HRMS (ESI⁺) calcd for C₁₂H₁₃BrN₃O₂ [M + H]⁺ 310.0186, found 310.0189. Anal. (C₁₂H₁₂BrN₃O₂) C, H, N.

Antimicrobial Assays—*G. lamblia* C6/WB (ATCC 50803), GS/M (ATCC 50580), BRIS/87/HEPU/713 (713),²⁴ BRIS/83/HEPU/106 (106)²⁵ were used as Mz-sensitive lines. The respective isogenic lines, 713-M3 and 106-21D₁₀, were employed as Mz-resistant lines.²⁴, ²⁵ C6/WB, 713, and 106 belong to *G. lamblia* assemblage A, while GS/M belongs to assemblage B. All lines were grown in TYI-S-33 medium supplemented with 10% bovine serum and 1 mg/mL bovine bile (Sigma) under anaerobic conditions.³⁶ The Mz-resistant lines were routinely cultured with 50 μM Mz but were grown without Mz for 2–3 days before experiments. Stocks of the test compounds (10 mM in DMSO) were diluted in PBS to 75 μM, and 1:3 serial dilutions were made in 40 μL TYI-S-33 medium in 96-well plates. Trophozoites were harvested in the mid-logarithmic growth phase and were added to the wells in a 10 μL volume at 1000–2000 cells/well (total volume 50 μL/well). Final compound concentrations ranged from 20 μM to 0.4 nM, covering a 5 log₁₀ range. Appropriately diluted solvent alone was used as a control. Cultures were grown for 2 days at 37 °C under anaerobic conditions (AnaeroPack-Anaero system, Remel). After incubation, cell growth and viability were determined with an ATP assay by adding 50 μL/well BacTiter-Glo microbial cell viability assay reagent (Promega) and measuring the luminescent signal in a microplate reader. The

50% effective concentration (EC_{50}), the drug concentration that inhibits *G. lamblia* growth by 50% compared to parallel cultures without added drugs, was determined by graphic extrapolation of the concentration–response curves. Antigiardial potency is expressed as negative \log_{10} value of the EC_{50} (pEC_{50}), with results calculated as mean \pm SE of three to four independent experiments. Initial studies showed that the results of the ATP assays correlated well with direct microscopic evaluation.

Cytotoxicity Assays—The human epithelial cell line HeLa (ATCC CCL-2) was maintained in DMEM, supplemented with 10% FBS, 5 mM HEPES, 50 U/mL penicillin, and 50 μ g/mL streptomycin, at 37 °C in 5% CO_2 /95% air. Compound stocks in DMSO were diluted in DMEM to a concentration of 375 μ M. Serial 1:3 dilutions were made in DMEM in 96-well plates (40 μ L/well), and 2000 HeLa cells were added per well in a 10 μ L volume. Final compound concentrations ranged from 100 μ M to 2 nM. Cells were cultured for 2 days, and viable cell numbers were determined with a dye reduction assay. For this, Alamar-Blue reagent (AbD Serotec) was added at 5 μ L/well, and cultures were incubated for 4 h, after which fluorescence was assayed in a microplate reader. The 50% inhibitory concentration (IC_{50}), the drug concentration that caused 50% loss of viability in the HeLa cultures compared to parallel cultures without added drugs, was determined by graphic extrapolation of the concentration–response curves. Toxicity is expressed as negative \log_{10} value of the IC_{50} (pIC_{50}), with results calculated as the mean \pm SE of three to four independent experiments.

Murine Giardia Infections—Adult C57BL/6 mice were obtained from The Jackson Laboratory (Bar Harbor, ME). For infections, trophozoites of *G. lamblia* GS/M were grown to mid-logarithmic growth phase and given by oral gavage at 10^7 /mouse in a 0.2 mL volume in TYI-S-33 growth medium. After 2 days (to allow establishment of infection), mice were given a test compound in 1% methylcellulose in PBS by oral gavage five times over a 3-day period. Controls received only methylcellulose/PBS. At day 5, the entire small intestine was removed and opened longitudinally, placed into 5 mL PBS, and cooled on ice for 10 min. After vigorous shaking to detach trophozoites, live *G. lamblia* were counted in a hemocytometer with a phase-contrast microscope. All animal studies were reviewed and approved by the UCSD Institutional Animal Care and Use Committee.

Electrochemical Measurements— $E_{1/2}$ values were measured by cyclic voltammetry, using a CH Instruments model 600c digital potentiostat with its standard software package. All measurements were conducted under Ar gas in a jacketed, one-compartment cell with a Pt wire counter electrode. For the nonaqueous CVs, a Au disk working electrode (~1 mm diameter) was used along with a Ag wire pseudoreference electrode. For the aqueous CVs, a glass carbon working electrode (~2 mm diameter) was used with a SCE reference electrode. Immediately before use, the working electrode was polished with 0.25 μ m diamond polishing paste, rinsed thoroughly with deionized water, polished with 0.05 μ m alumina paste, rinsed again with deionized water, then rinsed with acetone and dried with a tissue. The electrolyte solution used for the nonaqueous CVs was 0.10 M NBu₄PF₆ in DMSO. Prior to use, the solid electrolyte was recrystallized three times from 95% ethanol, dried overnight in vacuum at 100 °C, and stored in a desiccator. The solvent, anhydrous grade DMSO (Aldrich, sure-seal), was passed through a short column of activated alumina directly into the cell. Ferrocene was added as an internal potential reference. For the aqueous CVs, the electrolyte solution was 0.1 M KCl in pH 7.0 phosphate buffer (0.1 M ionic strength). For all experiments, oxygen was removed by bubbling Ar gas through the solution prior to making measurements. The temperature was controlled by using a circulating water bath to run 25 °C water through the outer cell jacket. In most experiments, 5 μ L of a 100 mM stock solution of the 5-NI compounds in DMSO was added to 3 mL of electrolyte solution in the cell to give a measurement concentration of 0.17 mM. CVs were recorded at 100 mV/s.

Acknowledgments

This work was supported by NIH U01 Cooperative Research Agreement AI75527 and the UCSD Digestive Diseases Research Development Center (DK80506). J.C.T. was supported by an NIH postdoctoral fellowship under the Ruth L. Kirschstein National Research Service Award program. P.H. was supported by a fellowship from the Swiss National Science Foundation (SSMBS; PASMA 114623). K.K. and L.V.A. received financial support from the CSU-LSAMP program funded by National Science Foundation, Grant HRD-0331537. We thank Taryn K. Fernandes, Cameron A. Collins, and M. Naomi King for help with the cyclic voltammetry studies.

References

1. Huang DB, White AC. An updated review on *Cryptosporidium* and *Giardia*. *Gastroenterol Clin North Am* 2006;35:291–314. viii. [PubMed: 16880067]
2. Thompson RC. Giardiasis as a re-emerging infectious disease and its zoonotic potential. *Int J Parasitol* 2000;30:1259–1267. [PubMed: 11113253]
3. Nash TE. Surface antigenic variation in *Giardia lamblia*. *Mol Microbiol* 2002;45:585–590. [PubMed: 12139606]
4. Berkman DS, Lescano AG, Gilman RH, Lopez SL, Black MM. Effects of stunting, diarrhoeal disease, and parasitic infection during infancy on cognition in late childhood: a follow-up study. *Lancet* 2002;359:564–571. [PubMed: 11867110]
5. Hanevik K, Hausken T, Morken MH, Strand EA, Morch K, et al. Persisting symptoms and duodenal inflammation related to *Giardia duodenalis* infection. *J Infect* 2007;55:524–530. [PubMed: 17964658]
6. Buret AG. Pathophysiology of enteric infections with *Giardia duodenalis*. *Parasite* 2008;15:261–265. [PubMed: 18814692]
7. Troeger H, Epple HJ, Schneider T, Wahnschaffe U, Ullrich R, et al. Effect of chronic *Giardia lamblia* infection on epithelial transport and barrier function in human duodenum. *Gut* 2007;56:328–335. [PubMed: 16935925]
8. Falagas ME, Walker AM, Jick H, Ruthazer R, Griffith J, et al. Late incidence of cancer after metronidazole use: a matched metronidazole user/nonuser study. *Clin Infect Dis* 1998;26:384–388. [PubMed: 9502459]
9. Wright JM, Dunn LA, Upcroft P, Upcroft JA. Efficacy of anti-giardial drugs. *Expert Opin Drug Saf* 2003;2:529–541. [PubMed: 14585063]
10. Anderson VR, Curran MP. Nitazoxanide: a review of its use in the treatment of gastrointestinal infections. *Drugs* 2007;67:1947–1967. [PubMed: 17722965]
11. Edwards DI. Nitroimidazole drugs—action and resistance mechanisms. I. Mechanisms of action. *J Antimicrob Chemother* 1993;31:9–20. [PubMed: 8444678]
12. Dan M, Wang AL, Wang CC. Inhibition of pyruvate-ferredoxin oxidoreductase gene expression in *Giardia lamblia* by a virus-mediated hammerhead ribozyme. *Mol Microbiol* 2000;36:447–456. [PubMed: 10792730]
13. Townson SM, Upcroft JA, Upcroft P. Characterisation and purification of pyruvate:ferredoxin oxidoreductase from *Giardia duodenalis*. *Mol Biochem Parasitol* 1996;79:183–193. [PubMed: 8855555]
14. Upcroft P, Upcroft JA. Drug targets and mechanisms of resistance in the anaerobic protozoa. *Clin Microbiol Rev* 2001;14:150–164. [PubMed: 11148007]
15. Salas-Herrera IG, Pearson RM, Johnston A, Turner P. Concentration of metronidazole in cervical mucus and serum after single and repeated oral doses. *J Antimicrob Chemother* 1991;28:283–289. [PubMed: 1778858]
16. Upcroft JA, Dunn LA, Wright JM, Benakli K, Upcroft P, et al. 5-Nitroimidazole drugs effective against metronidazole-resistant *Trichomonas vaginalis* and *Giardia duodenalis*. *Antimicrob Agents Chemother* 2006;50:344–347. [PubMed: 16377707]
17. Upcroft JA, Campbell RW, Benakli K, Upcroft P, Vanelle P. Efficacy of new 5-nitroimidazoles against metronidazole-susceptible and -resistant *Giardia*, *Trichomonas*, and *Entamoeba* spp. *Antimicrob Agents Chemother* 1999;43:73–76. [PubMed: 9869568]
18. Benakli K, Kaafarani M, Crozet MP, Vanelle P. Competition between C- and O-alkylation reactions in 5-nitroimidazole series: influence of nucleophile. *Heterocycles* 1999;51:557–565.

19. Dupau P, Epple R, Thomas AA, Fokin VV, Sharpless KB. Osmium-catalyzed dihydroxylation of olefins in acidic media: old process, new tricks. *Adv Synth Catal* 2002;344:421–433.
20. Narisada M, Horibe I, Watanabe F, Takeda K. Selective reduction of aryl halides and alpha, beta-unsaturated esters with sodium-borohydride cuprous chloride in methanol and its application to deuterium labeling. *J Org Chem* 1989;54:5308–5313.
21. Ishihara M, Togo H. An efficient preparation of 2-imidazolines and imidazoles from aldehydes with molecular iodine and (diacetoxyiodo) benzene. *Synlett* 2006:227–230.
22. Dandapani S, Jeske M, Curran DP. Synthesis of all 16 stereoisomers of pinesaw fly sex pheromones. Tools and tactics for solving problems in fluorine mixture synthesis. *J Org Chem* 2005;70:9447–9462. [PubMed: 16268620]
23. Kawasaki S, Fujita T, Toyota K, Yoshifuji M. Preparation and properties of fluorenylidene(phenyl) phosphines bearing bulky groups with electron-donating substituents in the ortho position on the phenyl group. *Bull Chem Soc Jpn* 2005;78:1082–1090.
24. Townson SM, Laqua H, Upcroft P, Boreham PF, Upcroft JA. Induction of metronidazole and furazolidone resistance in *Giardia*. *Trans R Soc Trop Med Hyg* 1992;86:521–522. [PubMed: 1475822]
25. Boreham PF, Phillips RE, Shepherd RW. Altered uptake of metronidazole in vitro by stocks of *Giardia intestinalis* with different drug sensitivities. *Trans R Soc Trop Med Hyg* 1988;82:104–106. [PubMed: 3176140]
26. Rouveix B. Clinical implications of multiple drug resistance efflux pumps of pathogenic bacteria. *J Antimicrob Chemother* 2007;59:1208–1209. [PubMed: 17507420]
27. Wright GD. Bacterial resistance to antibiotics: enzymatic degradation and modification. *Adv Drug Delivery Rev* 2005;57:1451–1470.
28. Liu SM, Brown DM, O'Donoghue P, Upcroft P, Upcroft JA. Ferredoxin involvement in metronidazole resistance of *Giardia duodenalis*. *Mol Biochem Parasitol* 2000;108:137–140. [PubMed: 10802327]
29. Muller J, Ley S, Felger I, Hemphill A, Muller N. Identification of differentially expressed genes in a *Giardia lamblia* WB C6 clone resistant to nitazoxanide and metronidazole. *J Antimicrob Chemother* 2008;62:72–82. [PubMed: 18408240]
30. Frontana C, Vazquez-Mayagoitia A, Garza J, Vargas R, Gonzalez I. Substituent effect on a family of quinones in aprotic solvents: an experimental and theoretical approach. *J Phys Chem A* 2006;110:9411–9419. [PubMed: 16869691]
31. Aguilar-Martinez M, Cuevas G, Jimenez-Estrada M, Gonzalez I, Lotina-Hennsen B, et al. An experimental and theoretical study of the substituent effects on the redox properties of 2-[(R-phenyl) amine]-1,4-naphthalenediones in acetonitrile. *J Org Chem* 1999;64:3684–3694. [PubMed: 11674498]
32. Leventis N, Rawaswdeh AMM, Zhang GH, Elder IA, Sotiriou-Leventis C. Tuning the redox chemistry of 4-benzoyl-N-methylpyridinium cations through para substitution. Hammett linear free energy relationships and the relative aptitude of the two-electron reduced forms for H-bonding. *J Org Chem* 2002;67:7501–7510. [PubMed: 12375985]
33. Legrand YM, Gray M, Cooke G, Rotello VM. Model systems for flavoenzyme activity: relationships between cofactor structure, binding and redox properties. *J Am Chem Soc* 2003;125:15789–15795. [PubMed: 14677969]
34. McDaniel DH, Brown HC. An extended table of Hammett substituent constants based on the ionization of substituted benzoic acids. *J Org Chem* 1958;23:420–427.
35. La-Scalea MA, Serrano SHP, Gutz IGR. Voltammetric behaviour of metronidazole at mercury electrodes. *J Braz Chem Soc* 1999;10:127–135.
36. Clark CG, Diamond LS. Methods for cultivation of luminal parasitic protists of clinical importance. *Clin Microbiol Rev* 2002;15:329–341. [PubMed: 12097242]

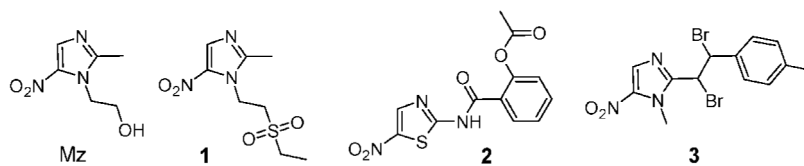


Figure 1.
5-Nitro heterocyclic compounds active against *Giardia*.

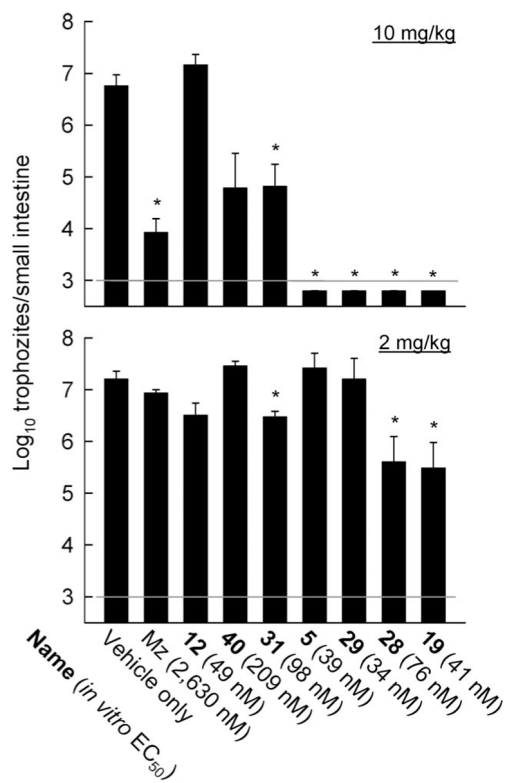


Figure 2.

In vivo potency of new 5-NI compounds against giardiasis. Adult C57BL/6 mice were infected orally with *G. lamblia* GS/M and given the indicated compounds at 10 or 2 mg/kg or vehicle only by oral gavage five times over a 3-day period starting 2 days after infection. Trophozoite numbers in the small intestine were determined 5 days after infection. Data are mean \pm SE of 3–7 animals. Asterisks designate a significant decrease ($p < 0.05$, t test) relative to infection controls given vehicle only. The gray line depicts the sensitivity of the assay. The *in vitro* activities of the respective compounds are taken from Tables 2–4.

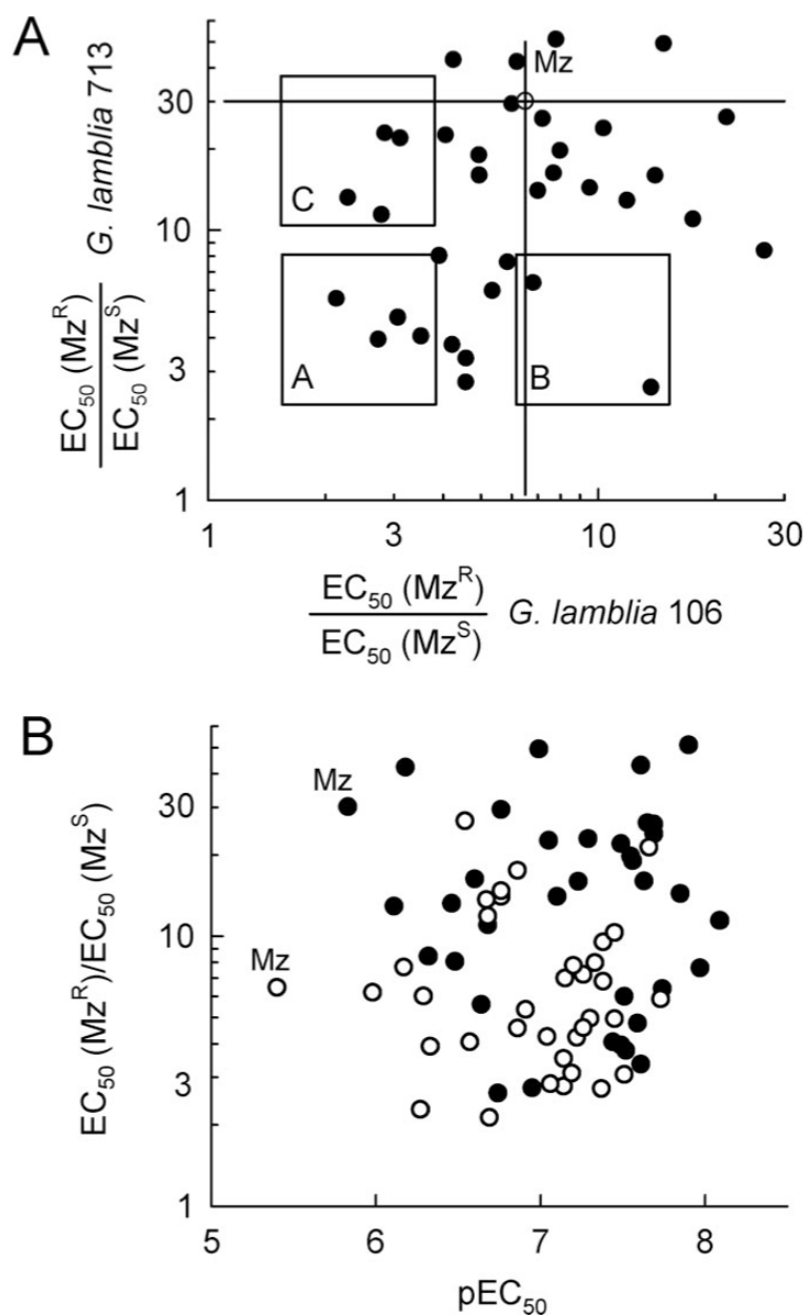


Figure 3.

Resistance profiles of new 5-NI derivatives. EC_{50} of all new compounds were determined for Mz^R and Mz^S lines of *G. lamblia* 713 and 106. The ability to overcome Mz resistance is expressed as the ratio of EC_{50} in the Mz^R line over EC_{50} in the Mz^S line and is plotted for each compound (A, closed circles). Mz (A, open circle) serves as the reference drug. Compounds were categorized arbitrarily into three groups to highlight their functional properties. In (B), resistance ratios for *G. lamblia* 713 (closed circles) and *G. lamblia* 106 (open circles) are plotted against the average antimicrobial activity against four Mz -sensitive lines for each drug, using the pEC_{50} values shown in Tables 2–4.

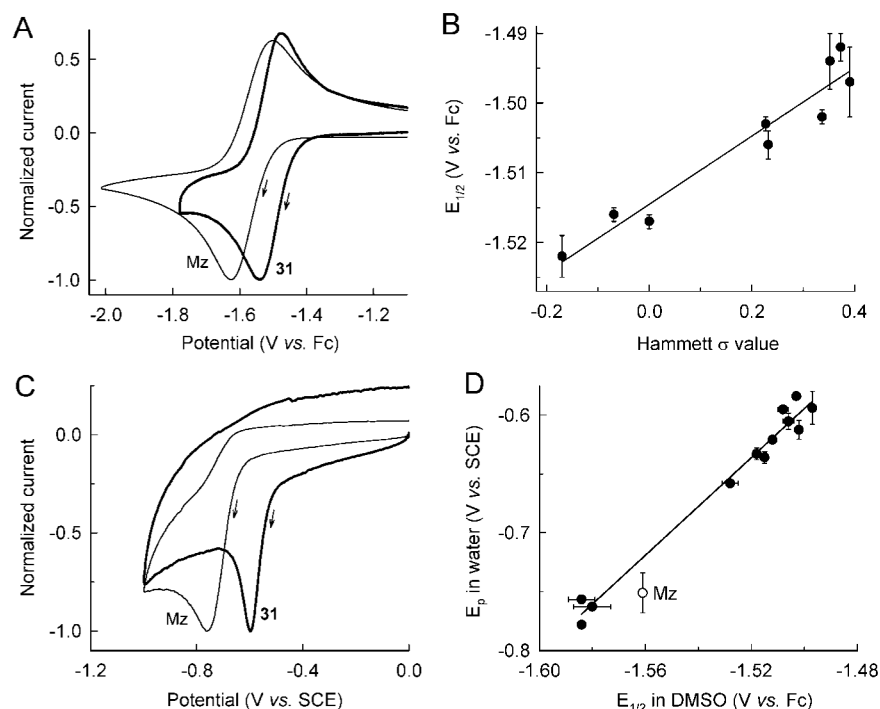


Figure 4.

Electrochemistry of new 5-NI compounds. 5-NIs were subjected to cyclic voltammetry in DMSO (A) or pH 7.0 water (C). Representative scans for Mz and the 3-thiophene compound **31** are shown. Potential is given relative to ferrocene (Fc) in DMSO or a saturated calomel electrode (SCE) in water. Current was normalized against peak cathodic current for each scan. The arrows indicate the scan direction. A summary of the electrochemical data is given in Table 6. $E_{1/2}$ values in DMSO were plotted against Hammett σ values of the 2-alkenylphenyl 5-NI compounds **5**, **7**, **8**, **11**, **12**, **14**, **15**, **18**, and **19** (B). $E_{1/2}$ values in DMSO were also plotted against E_p values in water for selected 5-NIs using the data in Table 6 (D). Data in (B) and (D) are the mean \pm SE of three to four experiments.

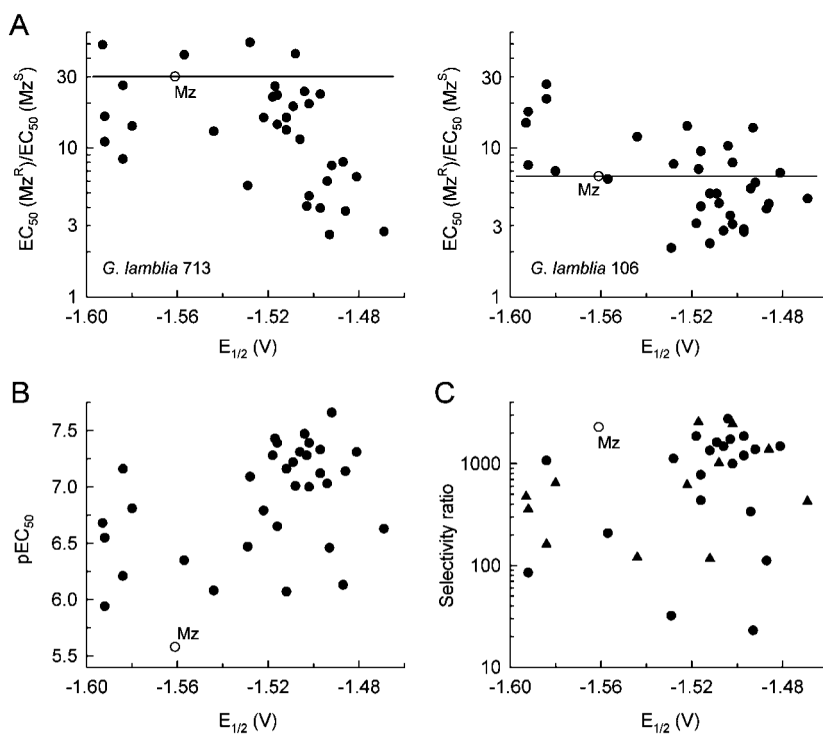
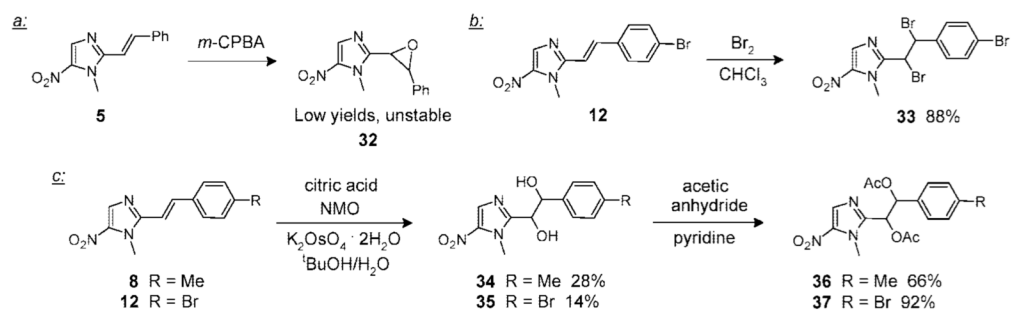
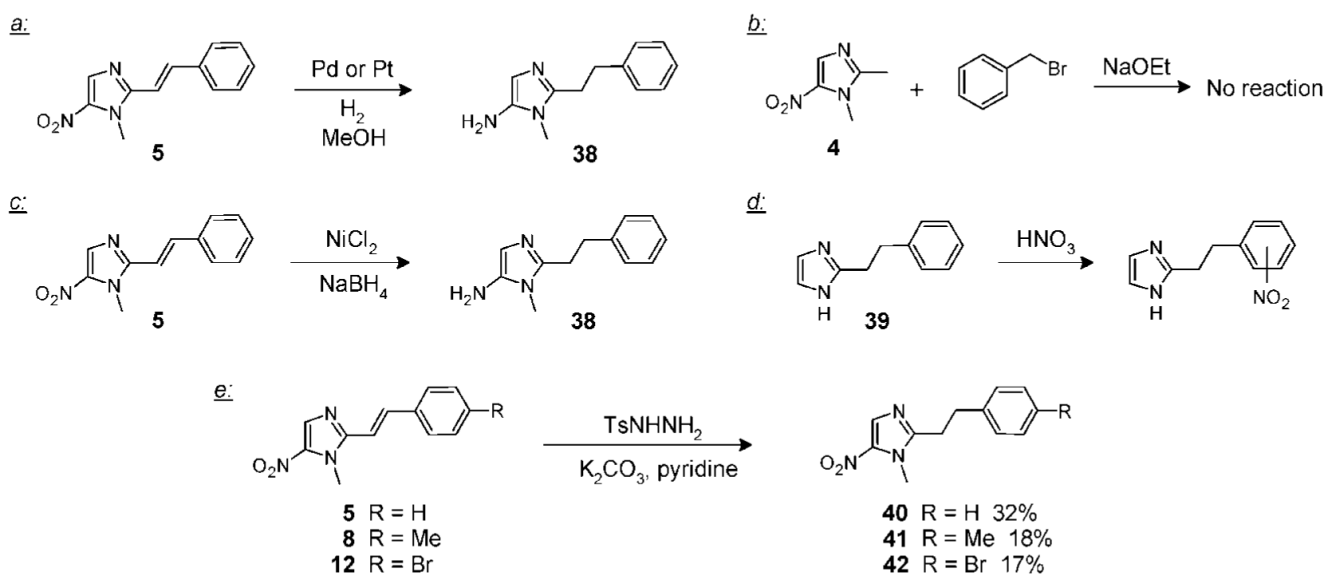


Figure 5. Relationship of redox potential and anti-giardial activity and selectivity for new 5-NI compounds. The redox potential in DMSO ($E_{1/2}$) of each new 5-NI was plotted against resistance ratios (A), overall anti-giardial activity (B), and selectivity ratio relative to HeLa cells (C). For compounds with limited aqueous solubility, the data points represent the ratio of EC_{50} and the highest test concentration ($100 \mu M$) and thus the minimum rather than exact selectivity ratio (closed triangles in C). Mz (open circles) is shown in all panels as the reference drug.



Scheme 1.



Scheme 2.

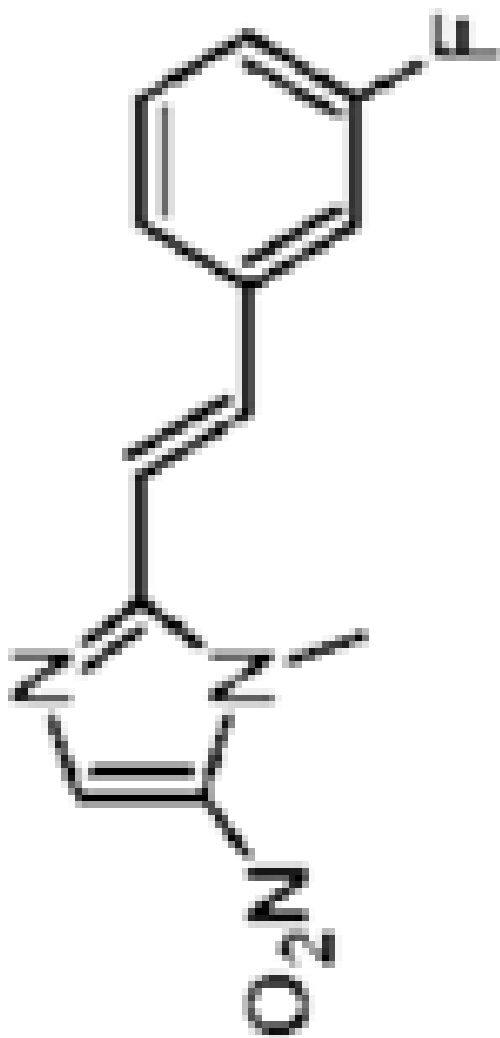


entry	Aldehyde	product	yield (%)
-------	----------	---------	-----------

15	3-fluoro-benzaldehyde		13
----	-----------------------	--	----

20

J Med Chem. Author manuscript; available in PMC 2010 July 9.



19



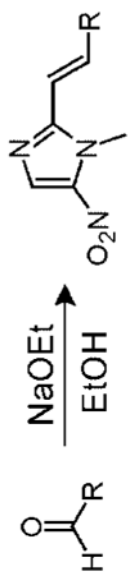
entry	Aldehyde	product	yield (%)
16	3-methoxy-benzaldehyde		32

32

23 16 3-methoxy-benzaldehyde

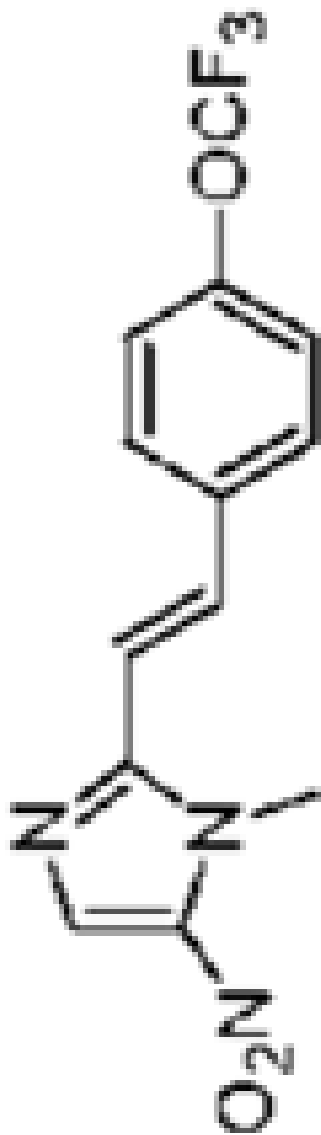
J Med Chem. Author manuscript; available in PMC 2010 July 9.

20



entry	Aldehyde	product	yield (%)
-------	----------	---------	-----------

42	17	4-trifluoro-methoxy-benzaldehyde	14
----	----	----------------------------------	----



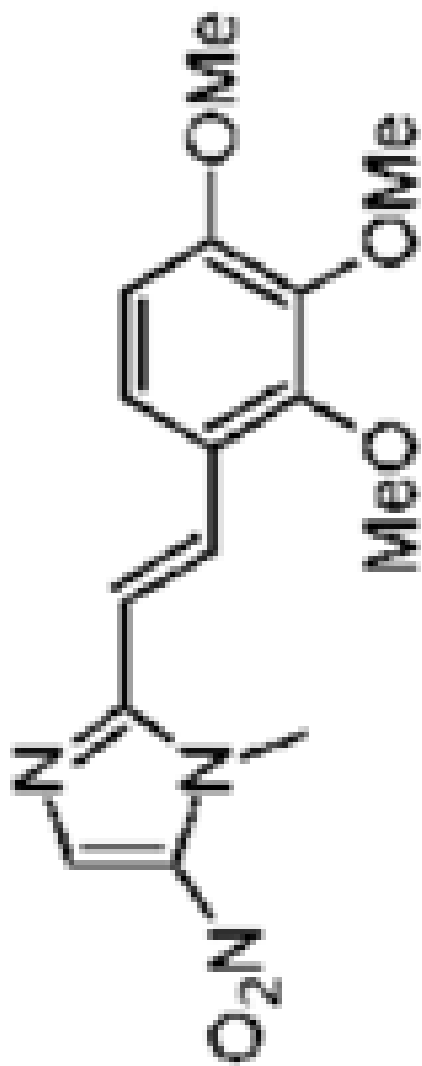
21



entry	Aldehyde	product	yield (%)
-------	----------	---------	-----------

16

22 18 2,3,4-trimethoxy-benzaldehyde



22

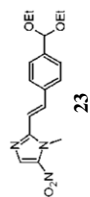


yield (%)

product

29 19 4-diethoxy-methyl-benzaldehyde

24



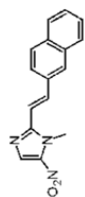


entry	Aldehyde	yield (%)	product	yield (%)
72	22	2-naphthyl-aldhyde		19

72

22 2-naphthyl-aldhyde

product



26

19

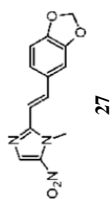


yield (%)

product

yield (%)entry/Aldehyde

31



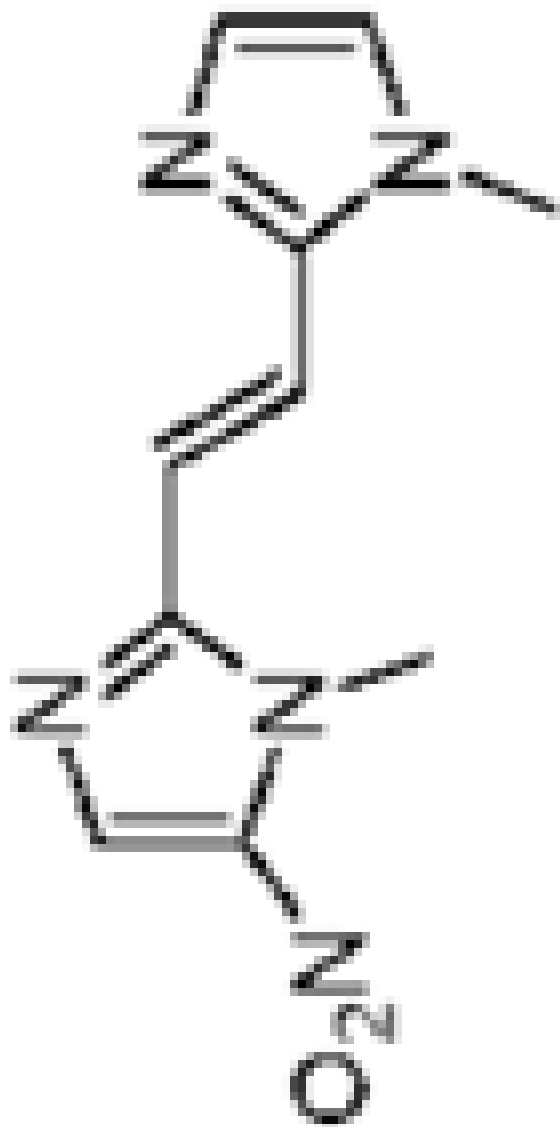
24 23 piperonal

J Med Chem. Author manuscript; available in PMC 2010 July 9.



entry	Aldehyde	product	yield (%)
-------	----------	---------	-----------

19	24	1-methyl-1-imidazole-2-carbaldehyde	77
----	----	-------------------------------------	----

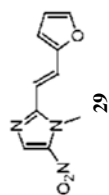


28



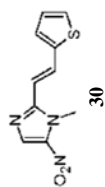
entry	Aldehyde	product	yield (%)
-------	----------	---------	-----------

15	25 furan-2-carbaldehyde		53
----	-------------------------	--	----



29

15	26 2-thiophene-carbaldehyde		23
----	-----------------------------	--	----



30



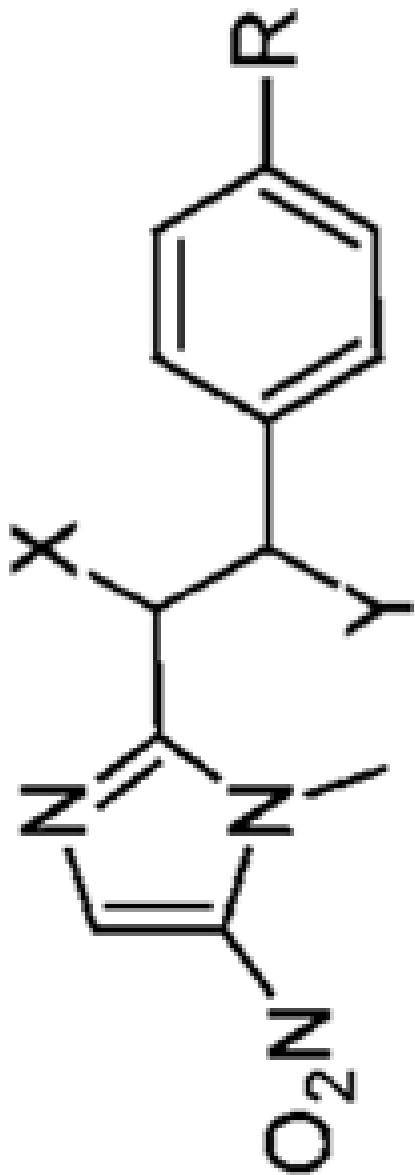
entry	Aldehyde	product	yield (%)
-------	----------	---------	-----------

20	27 3-thiophene-carbaldehyde	<p>31</p>	22
----	-----------------------------	-----------	----

J Med Chem. Author manuscript; available in PMC 2010 July 9.

Table 2

Antigiardial Potency and Toxicity of New 5-NI Alkanes

Activity against *G. lamblia*^a

entry	name	X	Y	R	EC ₅₀ (nM)	pEC ₅₀ (Mean ± SE)	toxicity in HeLa cells, ^b pIC ₅₀ (mean ± SE)	selectivity ratio, ^c IC ₅₀ /EC ₅₀
1	3	Br	Br	Me	65	7.19 ± 0.15	4.95 ± 0.06	174
2	33	Br	Br	Br	347	6.46 ± 0.15	5.10 ± 0.15	23
3	34	OH	OH	Me	832	6.08 ± 0.15	<4.00	> 120
4	35	OH	OH	Br	447	6.35 ± 0.19	4.04 ± 0.04	208
5	36	OAc	OAc	Me	316	6.50 ± 0.19	<4.00	> 319
6	37	OAc	OAc	Br	224	6.65 ± 0.16	4.01 ± 0.01	436
7	40	H	H	H	209	6.68 ± 0.18	<4.00	> 474
8	41	H	H	Me	282	6.55 ± 0.25	<4.00	> 357
9	42	H	H	Br	1148	5.94 ± 0.33	4.01 ± 0.01	85
10	Mz				2630	5.58 ± 0.09	2.22 ± 0.08	2291

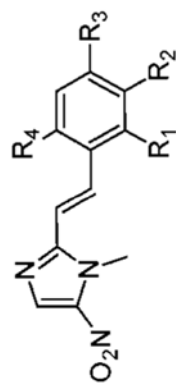
^a Activity against *G. lamblia* was determined as EC₅₀, the compound concentration that inhibited growth of *G. lamblia* by 50% over the assay period, and is expressed as negative log₁₀ value of the EC₅₀ (pEC₅₀). Higher pEC₅₀ values reflect greater potency. Data are mean ± SE of the average pEC₅₀ of four different *G. lamblia* isolates (WB/C6, GS/M, 106, and 713). The average pEC₅₀ for each individual isolate is based on the results of three to four separate experiments. Mean EC₅₀ was calculated from the mean combined pEC₅₀ for all four isolates.

^b Toxicity against HeLa cells was determined as IC₅₀, the compound concentration that killed 50% of HeLa cells in the cytotoxicity assays, and is expressed as negative log₁₀ value of the IC₅₀ (pIC₅₀), with higher values reflecting greater toxicity. Data are the mean ± SE of the results of three separate experiments.

^c Selectivity ratio, the ratio of IC₅₀ to EC₅₀, reflects the relative selectivity of compound potency against *Giardia* compared to toxicity in HeLa cells, with higher ratios indicating greater selectivity for the parasite.

Table 3

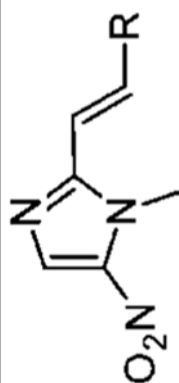
Antigiardial Potency and Toxicity of New 5-NI Alkenes



entry	name	activity against <i>G. lamblia</i> ^a						selectivity ratio, ^a IC ₅₀ /EC ₅₀	
		R1	R2	R3	R4	EC ₅₀ (nM)	pEC ₅₀ (mean ± SE)		toxicity in HeLa cells, ^a pIC ₅₀ (mean ± SE)
1	5	H	H	H	H	39	7.41 ± 0.12	<4.00	>2570
2	6	Me	H	H	H	69	7.16 ± 0.22	4.03 ± 0.03	1349
3	7	H	Me	H	H	40	7.40 ± 0.16	4.51 ± 0.24	776
4	8	H	H	Me	H	162	6.79 ± 0.17	<4.00	>617
5	9	Me	H	Me	Me	339	6.47 ± 0.15	4.96 ± 0.12	32
6	10	Br	H	H	H	49	7.31 ± 0.20	4.14 ± 0.13	1479
7	11	H	Br	H	H	47	7.33 ± 0.20	4.06 ± 0.06	1862
8	12	H	H	Br	H	49	7.31 ± 0.27	4.14 ± 0.10	1479
9	13	Cl	H	H	H	72	7.14 ± 0.15	<4.00	>1380
10	14	H	Cl	H	H	22	7.66 ± 0.18	4.52 ± 0.14	1380
11	15	H	H	Cl	H	52	7.28 ± 0.10	4.04 ± 0.05	1738
12	16	Cl	H	Cl	H	234	6.63 ± 0.22	<4.00	>427
13	17	I	H	H	H	60	7.22 ± 0.17	<4.00	>1660
14	18	H	I	H	H	93	7.03 ± 0.16	4.50 ± 0.23	339
15	19	H	F	H	H	41	7.39 ± 0.15	<4.00	>2455
16	20	H	OMe	H	H	155	6.81 ± 0.25	<4.00	>646
17	21	H	H	OCF ₃	H	741	6.13 ± 0.21	4.08 ± 0.09	112
18	22	OMe	OMe	OMe	H	617	6.21 ± 0.27	<4.00	>162
19	23	H	H	CH(OEt) ₂	H	52	7.28 ± 0.18	4.01 ± 0.01	1862
20	24	Ph	H	H	H	851	6.07 ± 0.23	<4.00	>117

^aActivity against *G. lamblia*, toxicity in HeLa cells, and selectivity ratios were determined and calculated as described in Table 2.

Table 4



entryname	activity against <i>G. lamblia</i> ^a		toxicity in HeLa cells ^d		selectivity ratio ^d (IC ₅₀ /EC ₅₀)
	EC ₅₀ (nM)	± SE	pEC ₅₀ (Mean)	± SE	
1	7.00	± 0.35	4.00	± 0.04	1,000

1,000

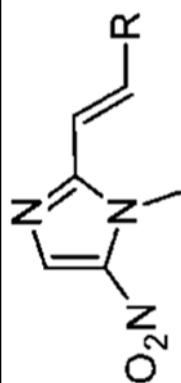
4.00 ± 0.04

7.00 ± 0.35

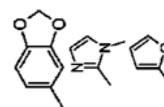
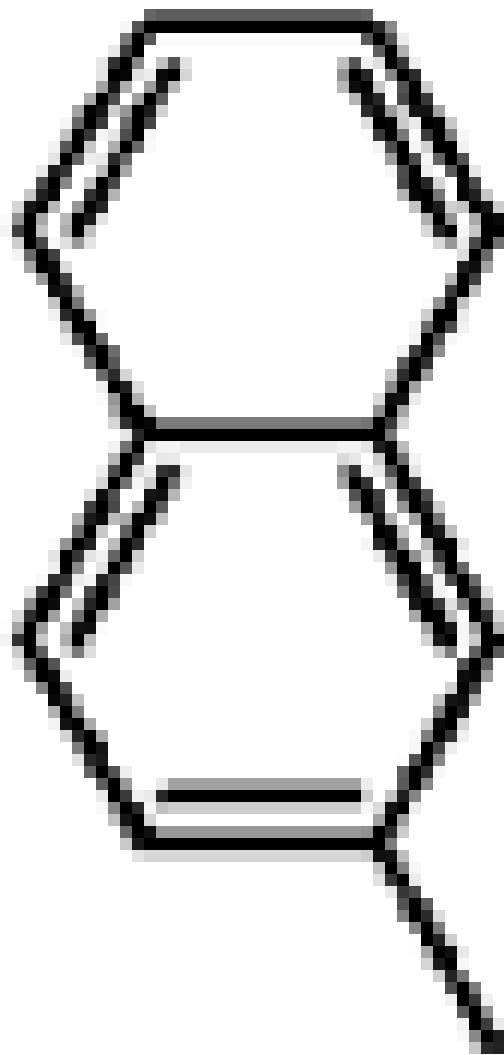
100

entryname

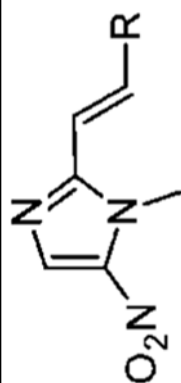
1 25



entryname	activity against <i>G. lamblia</i> ^a		toxicity in HeLa cells ^d		selectivity ratio ^d (IC ₅₀ /EC ₅₀)
	EC ₅₀ (nM) ± SE	pEC ₅₀ (Mean ± SE)	EC ₅₀ (nM) ± SE	pEC ₅₀ (Mean ± SE)	
2	60	7.22 ± 0.24	4.01 ± 0.01	1.622	



3	27	69	7.16 ± 0.34	4.13 ± 0.10	1.072
4	28	76	7.12 ± 0.12	4.04 ± 0.04	1.202
5	29	34	7.47 ± 0.08	4.03 ± 0.03	2.754

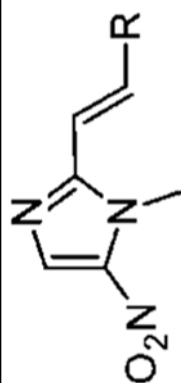


entryname	activity against <i>G. lamblia</i> ^a		toxicity in HeLa cells ^d		selectivity ratio ^d (IC ₅₀ /EC ₅₀)
	EC ₅₀ (nM) ± SE)	pEC ₅₀ (Mean ± SE)	EC ₅₀ (nM) ± SE)	pEC ₅₀ (Mean ± SE)	
6	81	7.09 ± 0.35	4.04 ± 0.05	1.122	

entryname

6 30

J Med Chem. Author manuscript; available in PMC 2010 July 9.



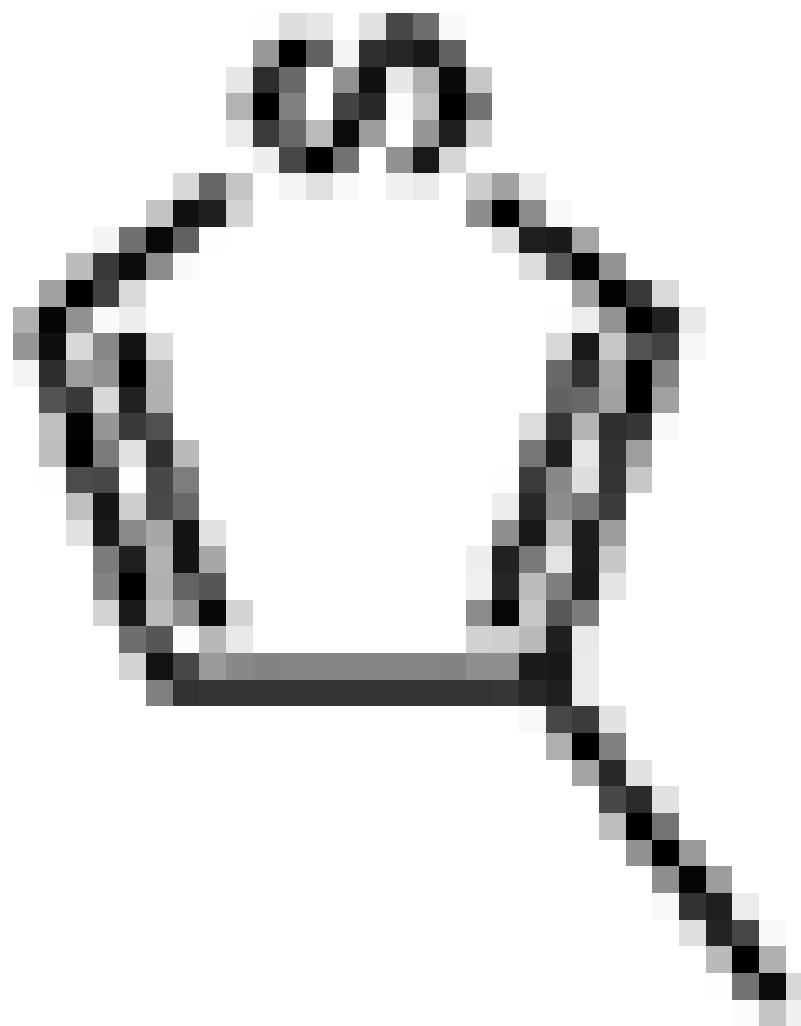
activity against <i>G. lamblia</i> ^a	toxicity in HeLa cells ^d	selectivity ratio ^d (IC ₅₀ /EC ₅₀)
pEC ₅₀ (Mean ± SE)	Mean IC ₅₀ (Mean ± SE)	
EC ₅₀ (nM) ± SE		

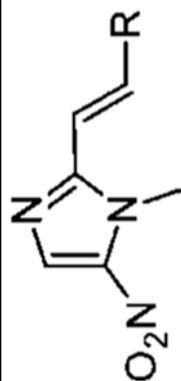
entryname

7 31

98 7.01 ± 0.27 <4.00 >1.023

r





activity against *G. lamblia*^a

toxicity in
HeLa cells^a

pEC₅₀ (Mean ± SE) selectivity ratio^a (IC₅₀/EC₅₀)

r

^a Activity against *G. lamblia*, toxicity in HeLa cells, and selectivity ratios were determined and calculated as described in Table 2.

Table 5

Activity of New 5-NIs against Mz-Resistant *G. lamblia*

group ^c	name	activity against <i>G. lamblia</i> 713, ^a pEC ₅₀ (mean ± SE)			activity against <i>G. lamblia</i> 106, ^a pEC ₅₀ (mean ± SE)			EC ₅₀ (Mz ^R)/EC ₅₀ (Mz ^S) ^b	
		Mz ^S	Mz ^R	Mz ^S	Mz ^R	Mz ^S	Mz ^R	<i>G. lamblia</i> 713	<i>G. lamblia</i> 106
A	Mz	5.83 ± 0.08	4.35 ± 0.12	5.40 ± 0.10	4.59 ± 0.08	30.20	6.46		
	9	6.64 ± 0.23	5.89 ± 0.02	6.69 ± 0.31	6.37 ± 0.24	5.59	2.13		
	11	7.49 ± 0.09	6.90 ± 0.12	7.37 ± 0.38	6.94 ± 0.11	3.95	2.73		
	15	7.44 ± 0.10	6.84 ± 0.10	7.14 ± 0.08	6.59 ± 0.22	4.06	3.52		
	19	7.59 ± 0.01	6.91 ± 0.09	7.51 ± 0.27	7.03 ± 0.10	4.76	3.07		
B	10	7.74 ± 0.10	6.93 ± 0.14	7.38 ± 0.18	6.55 ± 0.43	6.40	6.81		
	33	6.74 ± 0.09	6.32 ± 0.51	6.67 ± 0.23	5.54 ± 0.23	2.62	13.67		
	12	8.09 ± 0.46	7.04 ± 0.39	7.14 ± 0.17	6.70 ± 0.21	11.43	2.78		
C	23	7.49 ± 0.09	6.15 ± 0.12	7.19 ± 0.20	6.70 ± 0.14	22.00	3.11		
	24	6.46 ± 0.18	5.34 ± 0.34	6.27 ± 0.27	5.91 ± 0.19	13.22	2.28		
	28	7.29 ± 0.21	5.93 ± 0.02	7.06 ± 0.15	6.60 ± 0.14	22.96	2.84		
	5	7.69 ± 0.10	6.28 ± 0.20	7.26 ± 0.24	6.40 ± 0.14	25.98	7.20		
other	13	7.52 ± 0.27	6.94 ± 0.16	7.22 ± 0.13	6.60 ± 0.30	3.77	4.22		
	29	7.69 ± 0.10	6.31 ± 0.19	7.45 ± 0.28	6.44 ± 0.09	23.95	10.32		
	31	7.61 ± 0.61	5.98 ± 0.06	7.04 ± 0.03	6.41 ± 0.06	42.93	4.25		
	36	6.76 ± 0.15	5.29 ± 0.03	6.29 ± 0.16	5.51 ± 0.11	29.51	6.00		
	40	6.99 ± 0.16	5.30 ± 0.07	6.76 ± 0.13	5.59 ± 0.18	49.25	14.73		

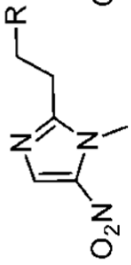
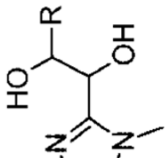
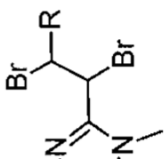
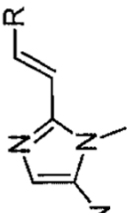
^a pEC₅₀ was determined for the respective Mz-sensitive (Mz^S) and Mz-resistant (Mz^R) lines of *G. lamblia*. Data are mean ± SE of three separate experiments.

^b The ratio of EC₅₀ in the Mz-resistant line to EC₅₀ in the isogenic Mz-sensitive line ("Mz resistance ratio") is a measure of the ability of a compound to overcome Mz resistance in the respective *G. lamblia* lines.

^c Group refers to the Mz resistance groups depicted in Figure 3A.

Electrochemical Properties of Modified 5-NIs

Table 6

group ^a	name	structure	R	mean ± SE	
				$E_{1/2}$ in DMSO (V vs Fc) ^b	E_p in water (V vs SCE) ^{b,c}
			I		
			II		
			III		
			IV		
40	1-methyl-5-NI	I	phenyl	-1.593 ± 0.002	ND
41		I	4-methylphenyl	-1.592 ± 0.003	ND
42		I	4-bromophenyl	-1.592 ± 0.003	ND
22		IV	2,3,4-trimethoxyphenyl	-1.584 ± 0.005	-0.757 ± 0.003
27		IV	1,3-benzodioxolyl	-1.584 ± 0.001	-0.778 ± 0.002
20		IV	3-methoxyphenyl	-1.580 ± 0.007	-0.763 ± 0.001
Miz				-1.561 ± 0.001	-0.751 ± 0.017
34		II	4-methylphenyl	-1.557 ± 0.001	ND
35		II	4-bromophenyl	-1.557 ± 0.001	ND
9		IV	2,4,6-trimethylphenyl	-1.544 ± 0.001	ND
30		IV	2-thiophenyl	-1.529 ± 0.001	ND
8		IV	4-methylphenyl	-1.528 ± 0.003	-0.658 ± 0.001
23		IV	4-dietoxymethylphenyl	-1.522 ± 0.003	ND
5		IV	phenyl	-1.518 ± 0.003	ND
7		IV	3-methylphenyl	-1.517 ± 0.001	-0.634 ± 0.004
6		IV	2-methylphenyl	-1.516 ± 0.001	-0.635 ± 0.003
24		IV	2-biphenyl	-1.512 ± 0.001	-0.621 ± 0.001
26		IV	2-naphthyl	-1.512 ± 0.001	ND
31		IV	3-thiophenyl	-1.509 ± 0.001	ND
12		IV	4-bromophenyl	-1.508 ± 0.002	-0.595 ± 0.001
29		IV	2-furanyl	-1.506 ± 0.002	-0.605 ± 0.007
15		IV	4-chlorophenyl	-1.504 ± 0.003	ND
25		IV	1-naphthyl	-1.503 ± 0.001	-0.584 ± 0.001
19		IV	3-fluorophenyl	-1.502 ± 0.004	ND
28		IV	1-methylimidazolyl	-1.502 ± 0.001	-0.613 ± 0.008
11		IV	3-bromophenyl	-1.497 ± 0.001	-0.594 ± 0.014
18		IV	3-iodophenyl	-1.497 ± 0.005	ND
33		III	4-bromophenyl	-1.494 ± 0.004	ND
14		IV	3-chlorophenyl	-1.493 ^d ± 0.004	ND
3		III	4-methylphenyl	-1.492 ± 0.002	ND
21		IV	4-trifluoromethoxyphenyl	-1.489 ^d ± 0.001	ND
13		IV	2-chlorophenyl	-1.487 ± 0.001	ND
10		IV	2-bromophenyl	-1.486 ± 0.004	ND
16		IV	2,4-dichlorophenyl	-1.481 ± 0.001	ND
		IV	2,4-dichlorophenyl	-1.469 ± 0.002	ND

^a Group refers to the Mz resistance groups in Figure 3A and Table 5.

^b Redox activation potential was determined by cyclic voltammetry in DMSO or water (pH 7.0). Half-wave potential ($E_{1/2}$) of the one-electron transfer reaction (0⁻1 reduction) was determined in DMSO, with ferrocene (Fc) as the internal reference. Peak potential, E_p , for the irreversible first electron reduction step was determined in water, using a saturated calomel electrode (SCE) as standard. Data are mean \pm SE of three to four separate experiments.

^c ND, not determined.

^d The $E_{1/2}$ values for these compounds are for the reversible wave, but given the different electrochemical response, these values can not be directly compared to the other $E_{1/2}$ values.